# Lead-Zinc Ore Deposits of the Tsushima Islands, Nagasaki Prefecture, with Special Reference to Shigekuma-type Mineralization

Shimada, Nobutaka
Faculty of Science, Kyushu University

https://doi.org/10.5109/1544181

出版情報：九州大學理學部紀要 : Series D, Geology. 23 (3), pp.417-480, 1977-02-25. Faculty of Science, Kyushu University
バージョン：
権利関係：

Mem. Fac. Sci., Kyushu Univ., Ser. D. Geol., Vol. XXIII, No. 3,
pp. 417-480, text-figs. 1-40, tables 1-18, February 25, 1977

# Lead-Zinc Ore Deposits of the Tsushima Islands, Nagasaki Prefecture, with Special Reference to Shigekuma-type Mineralization

Nobutaka SHIMADA

## Abstract

Lead-zinc ore deposits of the Tsushima Islands have been studied in terms of geology and mineralogy in order to reveal the essential factors contributed to localize the ore deposits, and also to establish spacial and paragenetic relations of mineralization concerned. The mineral assemblage, the variation of chemical compositions of minerals, and the characteristics of zonality have been discussed, so that the formation mechanism of the Shigekuma-type mineralization in Kamishima (North Tsushima) is clarified in comparison with that of the Taishu-type one in Shimojima (South Tsushima).

The geologic feature of the insular province is characterized with a thick pile of mudstone and sandstone of the Taishu Group, which deposited under the deltaic to shallow sea environments in late Oligocene to early Miocene. The group shows rather intensively folded structure and extensive fracturing as a result of a tectonic movement during the period of late Daijima to Nishikurosawa stages which acted in cooperation with both Mizuho and Takachiho orogenies.

The Taishu Group was intruded by sills and dikes of plagiophyre, quartz porphyry, dolerite and rhyolite, and by bosses and cryptobatholiths of biotite granite, just before and after the tectonic movement. The series of ore mineralization was probably formed in the period of Onnagawa stage, middle Miocene, being closely related to the granite intrusion.

All the ore deposits take the form of fissure-filling veins and are distributed in eight areas, namely, Sago, Nita-Miné, and Kin areas in Kamishima, and Ohfunakoshi, Izuhara, Sasu (Taishu mine), Tsutsu and Yora areas in Shimojima. They are impreganted in shear fractures along N-S and NE faults, and also in tension fractures along NW faults. The former fractures are well developed in the western part of Tsushima, where the folding is more intense, and the latters are dominant in the eastern part, especially around the axes of anticlinoria. The formation of fractures and the ore localization are controlled not only by lithofacies but also by the primary sedimentary structure. Although every ore deposit forms in the same kinds of fracture system, and is composed principally of lead-zinc-iron sulfide and carbonate minerals, ore deposits in Kamishima (Shigekuma-type) are distinct in some characters from those in Shimojima (Taishu-type).

Characteristics of the Shigekuma-type deposits are: 1) The mineralization started with deposition of Zn-Fe stage, followed by Cu-Ag and Pb stages, and ended in Fe-carbonate stage. 2) Relations between the distribution of minerals in each stage and the inter-mineralization fracturing indicate that ore-foming solutions with different compositions ascended along fissures repeatedly, while

Manuscript received September 10, 1976.

fracturing was taken place under a serial stress condition. This mineralization corresponds to the stage by stage zonality, especially to the tectonic opening-type in its zonality in SMIRNOV's sense. 3) No composition relations of main constituent minerals are observed with depth in each area of mineralization stage. 4) There crop out no acidic igneous rocks around the deposits, which can be related to the mineralization. 5) Homogenization temperatures of fluid inclusions show 208° to 222°C.

Remarkable features of the Taishu-type ore deposits are: 1) Mineralization was derived primarily in three stages, namely, Co-As, Fe-Zn-Pb, and rejuvenation stages. 2) All the ore deposits including 35 deposits in five areas are characterized by the higher temperature mineral assemblage, compared to the Shigekuma-type deposits. 3) These features are summarized with a serial mineralization which can be ascribed to an intimate association of the 12-million-year biotite granite. 4) The configuration of ores in the Co-As stage shows a district zoning with distance from granite, and that in the Fe-Zn-Pb stage clearly indicates a deposition-type zonality in the classification of facies zonality.

The Shigekuma-type deposit is concluded as a product of coprecipitation with boiling and throttling of ore-forming solutions under far from equilibrium, because of the primarily disturbed structures of ore and gangue minerals and the remarkable variations of chemical compositions of vein-forming minerals.

## Contents



## I. Introduction

Tsushima comprises two mainlands, Kamishima and Shimojima, besides a number of neighbouring islets. In the insular province, there occur many metalliferous ore deposits, chiefly lead-zinc veins or lodes. Earliest known production is of silver ore from Kashine, Shimojima in 674 A.D., which probably corresponds to the Taishu mine at present. Argentian galena ores were selectively mined and silver was probably refined by the cupellation method, until the early 17th century. Zinc ore, which had been estimated to be valueless for a long time, was firstly mined with lead ores at nearly the same place by the Sasu Mining Company in 1903, and followed by the C. Favre-Brandt Company in 1908. Zinc production was over one thousand metric ton until 1919.

In 1941, the Toho Zinc Company started work at the Taishu mine, and produced about five million metric tons of lead-zinc raw ores until 1973, when the production ceased. While, the Shirogane Mining Company exploited the Taishu-Shigekuma mine at Sago, Kamishima in 1963, and produced about sixty-

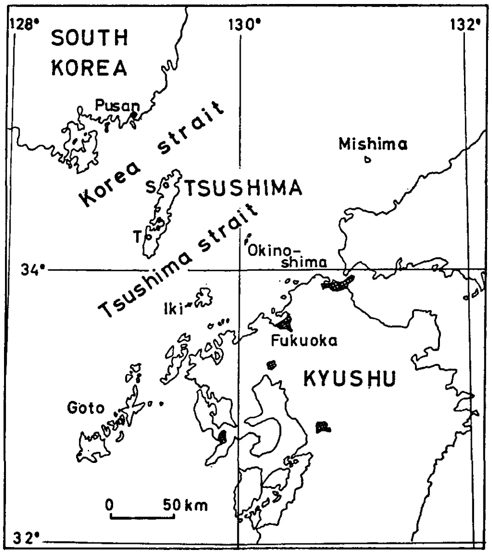


Fig. 1. Index map of the Tsushima Islands.
S: Taishu-Shigekuma mine, T: Taishu mine.

five thousand metric tons of silver-lead-zinc raw ores in nine years (Fig. 1).

The present writer has had opportunities to study the geology and ore deposits of these mines and also a number of small and closed mines around them (SHIMADA, 1971a, b, 1973a, b; SHIMADA and HIROWATARI, 1972; SHIMADA and WATANABE, 1973). Although numerous investigators have presented data and concepts pertinent to the structural control for the vein system, mineral zoning, and fluid inclusions of the deposits of the Taishu mine, the genesis of the deposits may still be disputable. This paper describes mineralogy and mineralization features of the lead-zinc ore deposits in Tsushima with some considerations on the geological factors for ore localization and also on the formation environment of ore deposits.

## II. Geology and ore deposits of Tsushima

### A. Geological setting

#### 1. *Outline of geology*

The geologic map of the Tsushima Islands is shown in Fig. 2, which is mainly compiled from MITI (1972–1974) and MATSUHASHI *et al.* (1970), and partly adapted by the present writer.

The geology of Tsushima consists primarily of the Taishu Group, which is divided stratigraphically into three conformable formations summing about or over 5,400 m in thickness.

The Lower Formation consists of thick mudstone intercalating medium to coarse grained sandstone beds at ten levels, and thin lapilli tuffs. It takes over 2,400 m thick, and the lower limit is unknown. The sandstone bed, taking less than 20 m thick, is mostly a fine alternating bed of thin sandstone and black shale.

The Middle Formation features dominant mudstone with some alternating beds of shale and banded sandstone. A thin lenticular layer of tuff occupies its basal part. The formation attains to a maximum thickness of about 1,600 m.

The Upper Formation takes more than 1,400 m thick and its upper limit is unknown. It is mainly composed of coarse grained arenitic sandstone with interbeded black mudstone and shale. It shows remarkable lateral change of lithofacies.

The Taishu Group is considered to have been deposited under deltaic to shallow sea environments from the following aspects. It shows a cycle of sedimentation with coarsening-upward, and marked cross-stratification (OKADA, 1969, 1970; OKADA and FUJIYAMA, 1970; MATSUMOTO, T., 1969). The slumping structure and scours are common in various horizons of the Upper and Lower Formations (KITAMURA, 1961; OKADA *et al*., 1971; NAGAHAMA, 1971). The direction of paleocurrent shows beautifully straight line toward the northeast in any horizons (NAGAHAMA, 1967; NAGAHAMA *et al*., 1966; OKADA, 1969; TAKAHASHI and MATSUHASHI, 1970). The thick formations of the Taishu Group may have been formed by a gradual shift of the sedimentation center northeastwards during the deltaic deposition.

The Taishu Group is intruded by some thick sheets of plagiophyre and quartz porphyry, and a number of dolerite dikes and bosses. It is also invaded by biotite granite mass, which crops out at Uchiyama and Hikage, the southern part, and is distributed beneath hornfels zone in the northeastern part of Shimojima. Neither hornfels nor granite is found in Kamishima. According to the results of an airborne prospecting, a cryptobasolith may be present at the depth of about 2,000 m off the east coast of Kamishima as shown in Fig. 4 (MITI, 1973). A small granite body may also be present in a shallow portion under Ohfunakoshi Peninsula (MITI, 1973).

Field observation suggests that plagiophyre selectively intruded into tuff beds or nearly equal horizons, and it was furthermore invaded by quartz porphyry to form complicated composit dikes. Both of them show sheet structures, but are folded together with sediments of the Taishu Group. Meanwhile, biotite granite gave thermal metamorphism to the sedimentary rocks and even to plagiophyre and quartz porphyry, to form biotite- or biotite-cordierite hornfels in the formers and spotted cordierite- or andalusite-hornfels in the latters. Altered dolerite dikes clearly intersect across quartz porphyry at Tsuyashima. Rhyolite exhibits the flow and spherulitic structures, and greyish white in color. It occurs as sheets at Otedo and Nezumijima. Its intrusion was probably simultaneous with that of biotite granite.

Hence, the sequence of the igneous activities in Tsushima is summarized as follows: volcanic eruption in the deposition time of the Taishu Group to form pyroclastic seams, the intrusion of plagiophyre and quartz porphyry before and during the tectonic movement, followed by dolerite intrusion, and then granite and rhyolite invasions.

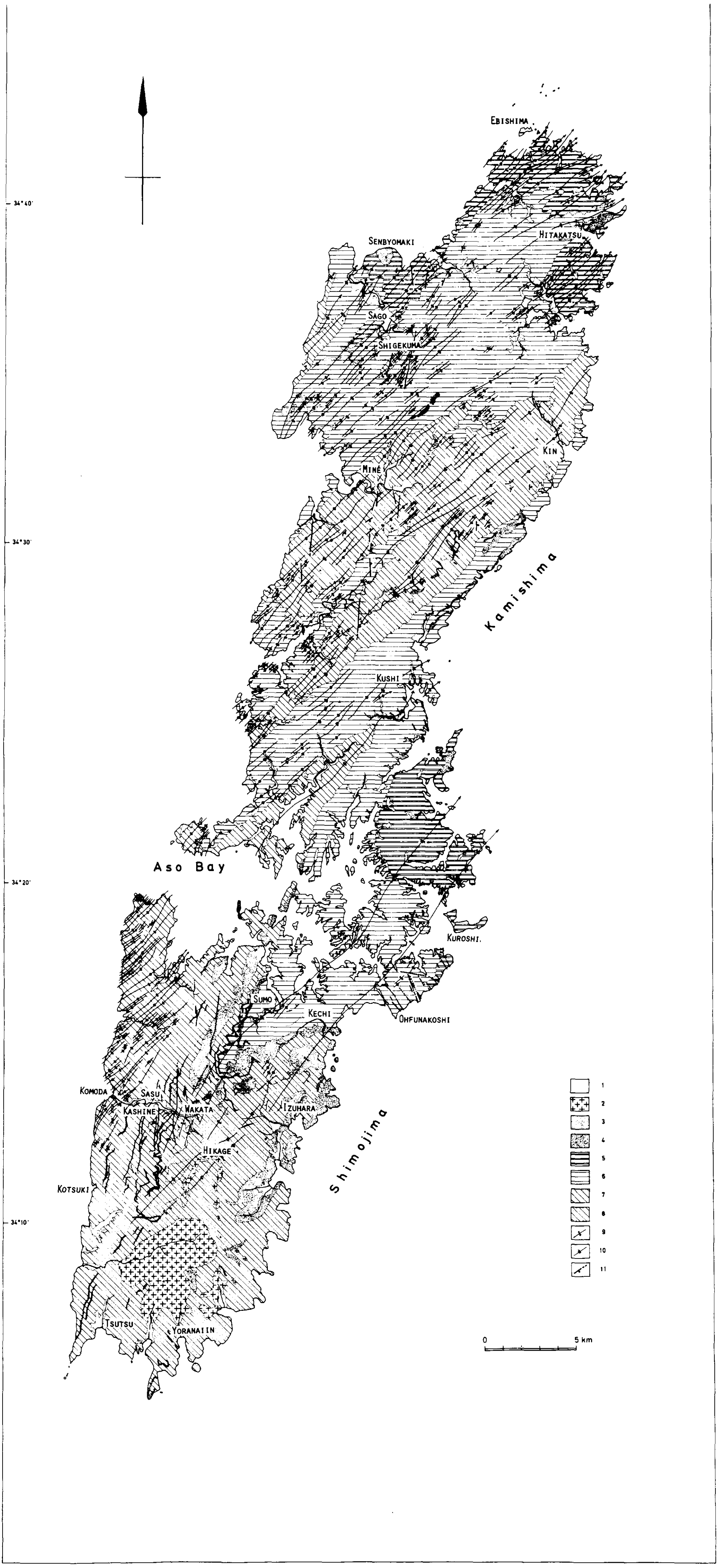


**Fig. 2. Geologic map of the Tsushima Islands.**
1: alluvium, 2: biotite granite, 3: dolerite and basic igneous rocks, 4: plagiophyre, quartz porphyry, and rhyolite, 5: Upper Formation of the Taishu Group, 6: Middle Formation, 7: Lower Formation, 8: hornfels zone (dotted area), 9: anticline, 10: syncline, 11: fault.

Table 1. Stratigraphic correlation of the Tertiary formations in Kyushu and Shimane Prefecture

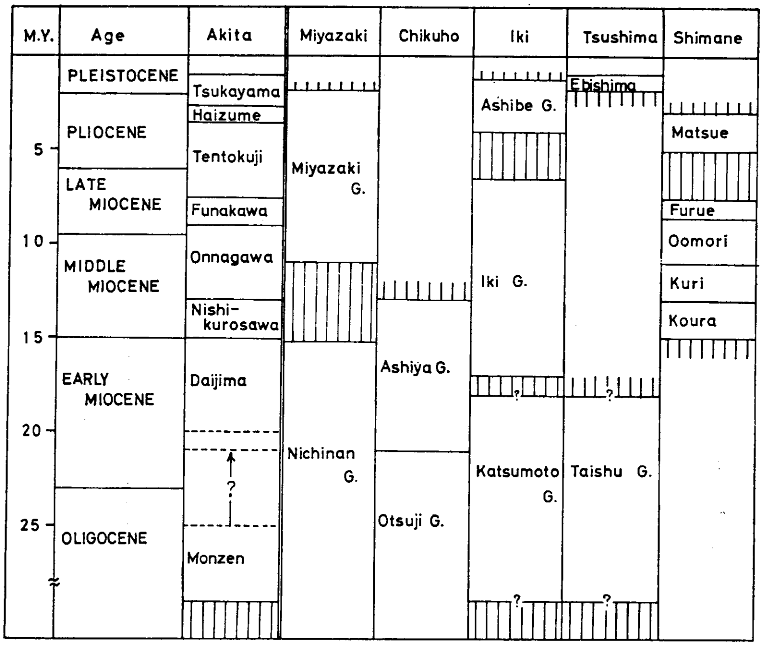


## 2. *Stratigraphic correlation*

Adopting a geological scale presented by IKEBE *et al.* (1971), the depositional age of the Taishu Group can be concluded as below by the following facts. 1) Correlation of Kotsuki flora from the lower part of the Lower Formation of the Taishu Group to the Sakito Flora in Northwest Kyushu (MATSUO, 1971). 2) Correlation of the upper part of the Lower Formation, which yields fossil flora (*Sabalites*), to the Otsuji stage in North Kyushu (TAKAHASHI, 1958). 3) Discovery of molluscs fossils (*Glycymeris, etc.*) from the upper part of the Lower Formation of the Taishu Group to the Ashiya Group in North Kyushu (TAKAHASHI and NISHIDA, 1975). 4) Biotite granite which invaded into the Taishu Group shows the age of 12 million years by K-Ar method (KAWANO and UEDA, 1966). Then, according to the stratigraphic correlation on the Tertiary systems in Kyushu presented by SHUTO (1969), the Taishu Group is considered to have been deposited in late Oligocene to early Miocene as shown in Table 1.

The Katsumoto Group of the Iki Islands is probably correlated to the Taishu Group from its lithofacies and the directions of paleocurrent (MATSUMOTO, T. *et al.*, 1962). The Group is mainly composed of sandstone-shale alternation, intercalating thin tuff bed. It makes the basement of the islands, and crops out in the northern part. Geological Research Group of Iki Islands (1973) also correlated the age of Iki Group to Oligo-Miocene.

The Okinoshima Islet is situated as the nearest neighbourland to Tsushima as well as Iki (Fig. 1), but it is composed of black shale and porphyrite sheet.

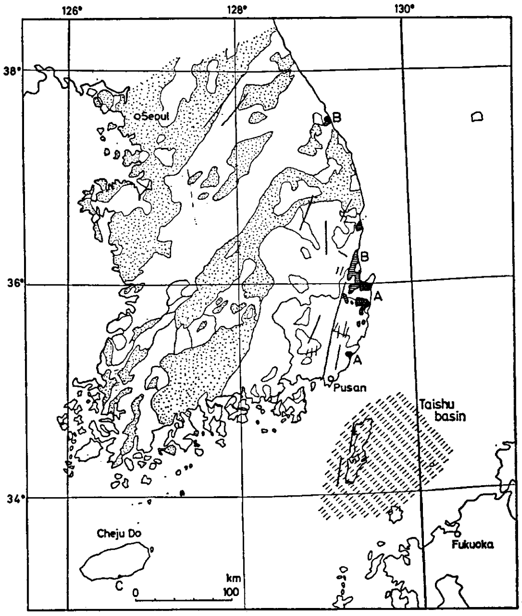


Fig. 3. Distribution of the "Taishu basin", and the Tertiary formations in Korea.
A: Yang-bug Group, B: Yeong-il Group, C: Seo-gui-po Formation. Dotted area: Precambrian Group.

The lithofacies is quite similar to that of the Taishu Group, and the age of porphyrite intrusion is estimated to be Miocene from the color of zircons (TSUJI, 1973; TAKAI, pers. commun.).

Therefore, the deposition basin of the Taishu Group is considered to have been widely distributed in a region including Tsushima, Iki and Okinoshima islands at least, as shown in Fig. 3.

The Tertiary system of Korea is known to be distributed snugly at the eastern part (Fig. 3), and is divided into three groups, namely, Yang-bug, Yeong-il, and Seo-gui-po Group (Geological and Mineral Institute of Korea, 1973). The Yang-bug Group is almost composed of non marine sediments and pyroclastic rocks, and may correspond to middle Miocene (KIM *et al.*, 1974). The Yeong-il Group is probably regarded to upper Miocene (K. TAKAHASHI, pers. commun.). The Seo-gui-po Formation distributed only in Cheju-do Islands is of Plio-Pleistocene. The geology and sedimentary environments of the groups are, however, distinct from those of the Taishu Group judging from the data available.

On the Ebishima Islet, which is located at the north-end of Kamishima, the Ebishima Formation is exposed as a small rock body which overlies the Upper Formation of the Taishu Group with unconformity. It consists wholly of porous biosparlite and biolithite, and is regarded to be Quaternary sediment (OKADA *et al.*, 1971).

3. *Geological structure*

The framework structure of the islands is controlled principally by some intensive folds, having axes nearly parallel to NE-SW direction and plunging gently northeastwards. Major folds are composed of six anticlinoria and five synclinoria, making the wave length of 5 to 10 km (Figs. 2 and 4). The second order of folding structure is well developed in the western part of the islands, showing its axial length within 1 km (Fig. 2). The preferential distribution of the second order folding seems to have been intimately controlled by the structure of the basement and also by the formation of a major fault developed in the sea area off the west coast of Tsushima. The fault is called "Korea Strait Tectonic Line", whose apparent throw is estimated over 1 km with a seismic prospecting (MURAUCHI, 1972).

Faults expressed on the islands are classified by their trends and properties into N-S, NE, and NW faults. The N-S faults are parallel to the elongation of "Korea Strait Tectonic Line", and are distributed in the central part of the islands. They usually have the strike of NNE-SSW to N-S, and the dip of 60° to 80° eastwards. Almost all of them are left handed strike-slip faults, and show the form of echelon accompanied by gouges within 1 m and sheared zones within 6 m in width. The NE faults are dip-slip or bedding-plane reverse faults, developed along the boundary between sandstone and mudstone around the wing part of folds. The NW faults exhibit nearly vertical dips with strikes of NNW to WNW. The faults are densely developed in Ohfunakoshi Peninsula, and are also found sporadically in the eastern part of the islands.

MATSUMOTO, T. (1969) suggested that the folding feature of the Taishu Group was Jura- or décollement-type. It implies that the basement is present in rather shallow portion under the Taishu Group, and is composed of highly competent bed with flat surface. However, the information about the basement has not yet been known, except seismic data and a gravity map by an air borne prospecting. According to MURAUCHI (1972), the Taishu Group having 1.9 km/sec propagation velocity is distributed to 0.5 km depth under the sea level, and the underlying bed having 3.3 km/sec is about 200 m thick. At about 2.1 km under the sea level, there may be crystalline rocks having 4.1 km/sec velocity. In a recent paper, TERASHIMA and TSUCHIYA (1976) suggested that high density basement exists beneath the Taishu Group, and it exhibits NE-SW trending step-like structure, and also N-S trending axis of flexure structure which sets up the bouderline between the eastern side nearly horizontal and the western side inclining twenty degrees to the west.

The facts described above may indicate that the tectonic movement on the Taishu Group had probably been made by a horizontal compressive force of NW-SE trend, which acted right angles to the general trend of folds. The force contributed the formation of fault systems in Tsushima, because the NW faults are tension fractures and the N-S and NE faults are shear ones, as described later.

4. *Igneous activity and tectonic movement*

The igneous activities in Tsushima are, as described above, characterized

Table 2. Correlation of igneous activity, tectonic movement, and mineralization of Tsushima

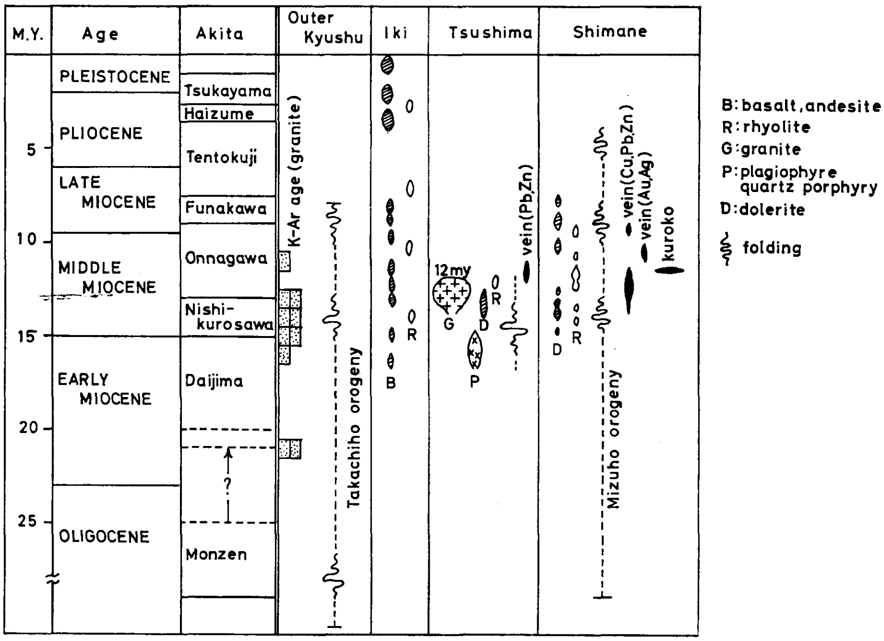


by intrusions of plagiophyre and quartz porphyry, dolerite, biotite granite, and rhyolite. As the deposition age of the Taishu Group is considered to be Oligocene to early Miocene, and K-Ar age of biotite granite indicates 12 million years, these igneous activities may have been taken place in early to middle Miocene, as shown in Table 2.

The tectonic movement may have brought out in early Middle Miocene, or Nishikurosawa stage, because plagiophyre and quartz porphyry are folded together with the Taishu Group, and also dikes of dolerite and rhyolite fill N-S and NW fractures. Biotite granite intruded into the crest of anticline and cooled down in the Onnagawa stage, or in the ending stage of the tectonism.

Following important facts, these igeneous activities and tectonic movement in Tsushima are found in relation to those in South Kyushu, Iki, and the "Green Tuff" region: Firstly, the age of granite in Tsushima coincides well with the ages of some granites in the Outer Zone of Kyushu. Secondly, dolerite and rhyolite intrusions in Tsushima happened in nearly the same period as those in the "Green Tuff" region. Thirdly, the period of the tectonic movement in Tsushima agrees with that of both Takachiho and Mizuho orogenies. Although the tectonic expression of the Takachiho orogeny in North Kyushu is rather weak (SHUTO, 1969), the tectonic movement in Tsushima may be regarded as a harmonic movement with both Takachiho and Mizuho orogenies. Lastly, as the mineralization in Shimojima associates intimately with biotite granite, its formation age may be early Onnagawa stage. The age may correspond to the formation ages of many vein-type and Kuroko deposits in "Green Tuff" region

(TATSUMI *et al.*, 1970; SATO, 1972; YAMAOKA, 1976), and also to those of Obira-type deposits in the Outer Zone of Kyushu (MIYAHISA, 1961).

The alignment of the ages of igneous activity, tectonic movement, and mineralization in Tsushima implies significant problems on the geohistory and metallogeny of Japan, and more precise data on the formation ages of ore deposits and detailed correlations among sedimentary basins are needed.

## B. Ore deposits of Tsushima

### 1. *Distribution of ore deposits*

In the Tsushima Islands, a lot of metalliferous ore deposits and non-metallic ones are distributed. Almost all of the former deposits are lead-zinc ones, which are distributed nearly all over the islands. Most of them were exploited largely by the Taishu mine and the Taishu-Shigekuma mine. The latters are pottery stone deposits, which are actively mined at Izuhara town (IWAO, 1958; SUZAKI *et al.*, 1970).

The distribution of metalliferous ore deposits in two mainlands, Kamishima and Shimojima, is divided into following eight areas as shown in Fig. 4.

**Kamishima**

1) Sago area: Iguchihama, Shigekuma, Nihongi, Chihira, Genju-Nakinaki, Nakanosae, and Miyama-Shigeeda.

2) Kin area: Kanayama.

3) Nita-Miné area: Koenosaka, Kaidokoro, Kasayama, Seta, Shikoe, and Miné-Kanayama.

**Shimojima**

4) Ohfunakoshi area: Ohfunakoshi, Konjobana, Ogata, Misaki, and Kuroshima.

5) Izuhara area: Nariaisai, Momijiyama, and Kamisaka.

6) Sasu (Taishu mine) area: Shiratake-Uwaban, Shiratake, Misumiyama-Higashi, Tsurue, Tsurue-Somen, Senninmabu-Somen, Misoge, Taisho, Showa, Nishikura, Sekinokuma, Kunoe, Kunoe-Somen, Akushidani, Akushidani-Uwaban, Tsuruketa, Motoyamamichi, Furukawa, Kune-Toobu, Aré, Shiinehama, Shiine, Tonohama, Amanohara, Urakochi-Somen, Shimobaru, and Shimoken.

7) Tsutsu area: Ozakiyama.

8) Yora area: Yoranaiin.

### 2. *Ore deposits in Kamishima*

In Kamishima, the denser distribution of lead-zinc ore deposits is recognized in Sago, Kin, and Nita-Miné areas as mentioned above. The ore deposits and outcrops are listed in Table 3, with the directions of veins and the constituent ore and gangue minerals.

Among the deposits, Shigekuma and Nihongi deposits in Sago area and Kanayama deposit in Kin area were recently exploited by the Taishu-Shigekuma mine, Shirogane Company. They are larger than any other closed deposits in

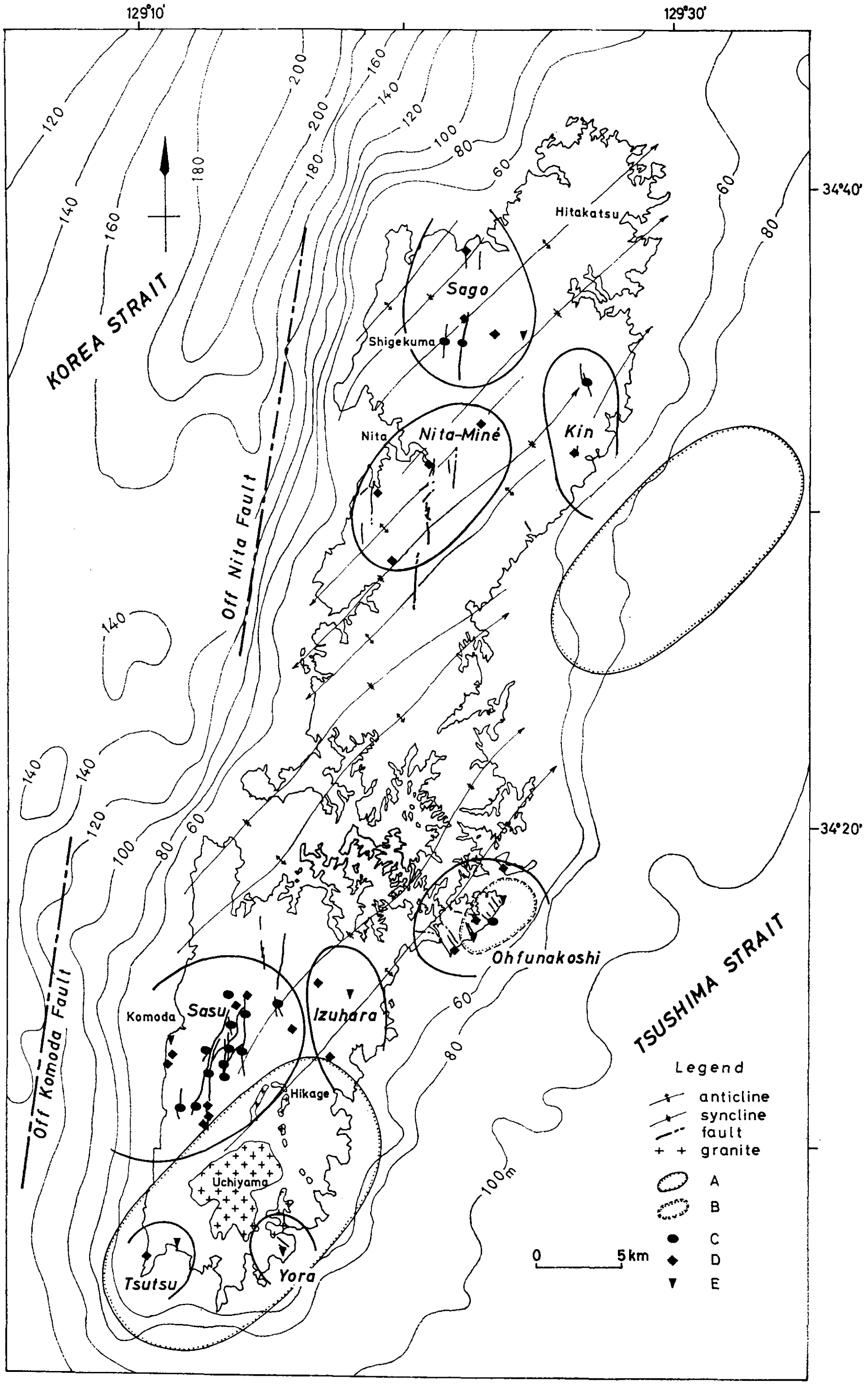

129°10'
129°30'
34°40'
34°20'
KOREA STRAIT
TSUSHIMA STRAIT
Off Nita Fault
Off Komoda Fault
Hitakatsu
Sago
Shigekuma
Nita
Nita-Mine
Kin
Komoda
Sasu
Izuhara
Ohfunakoshi
Hikage
Uchiyama
Tsutsu
Yora
120
140
160
180
200
100
80
60
100m
Legend
anticline
syncline
fault
granite
A
B
C
D
E
0
5km

Table 3. Ore deposits and outcrops in Kamishima

| Area | Ore deposit & Outcrop | Strike & dip of vein | Wall rock | Ore & gangue minerals |
|---|---|---|---|---|
| SAGO | Iguchihama | NS, 80°E. | Alt. | Sph, Gn, Cp, Py, Tet, Q, Ank. |
| | Shigekuma | N50-60°E, 20-70°N or S, N0-30°E, 60-80°E. | Alt. | Sph, Gn, Cp, Tet, Bour, Ull, Sid, Q, Ank. |
| | Nihongi | N5°W-N20°E, 50-90°E, N10-40°W, 55-75°W, N60°W-N85°E, 80°N. | Alt. Ss. | Sph, Py, Gn, Cp, Tet, Sid, Q, Ank. |
| | Chihira | N60°E, 80°N or S, | Alt. | Sph, Gn, Q, Ank. |
| | Genju-Nakinaki | N50-70°E, 40-70°S. | Alt. | Sph, Gn, Cp, Tet. Q, Ank. |
| | Nakanosae | N72°E. 80°N. | Alt. | Q, Sph, Gn, Cp, Ank. |
| | Miyama-Shigeeda | N60°W, 88°S. | Dol. | Q, Ank. |
| | Kamigasai Outcorp | N64°E, 76°S. | Alt. | Sph, Q, Ank. |
| | Kamigasaiguchi Outcrop | N50-90°W, 23-66°N. | Alt. | Sph, Gn, Tet, Q, Ank. |
| KIN | Kanayama | N0-35°W, 50-70°E. | Dol. Ss. | Sph, Py, Gn, Sid, Q, Ank. |
| | Koonokiyama Outcrop | N75°W, 55°S. | Dol. | Sph, Gn, Q, Ank. |
| NITA-MINÉ | Koenosaka | N30°E, 70°N. | Mud. | Q, Ank, Sph, Gn. |
| | Kaidokoro | N20-25°E, 70°E, N50°E, 20°S. | Mud. | Q, Ank, Sph, Gn. |
| | Kasayama | N37°E, 67°W. | Alt. | Q, Ank, Sph, Gn. |
| | Seta | N52°E, 50°NW. | Alt. | Lim. |
| | Shikoe | N30°W, 90°. | Dol. | Q, Lim. |
| | Miné-Kanayama | N71°W, 40°N. | Dol. | Gn, Q. |
| | Miné-Nakazato Outcrop | N80-85°E, 52-90°S. | Dol. | Q, Gn, Cer. |

Alt., alternation; Ss., sandstone; Dol., dolerite; Mud., mudstone; Sph, sphalerite; Gn, galena; Cp, chalcopyrite; Py, pyrite; Tet, tetrahedrite; Bour, bournonite; Ull, ullmannite; Sid, siderite; Q, quartz; Ank, ankerite; Lim, limonite; Cer, cerussite.

Fig. 4. The distibution of ore deposits in Tsushima.
A: magnetic anomaly showing the extension of granite boss in the depth of about 2,000 m, B: magnetic anomaly showing the location of granitic body in the shallow portion, C: ore deposit exploited recently, D: ore deposit mined long ago, E: outcrop of ores.

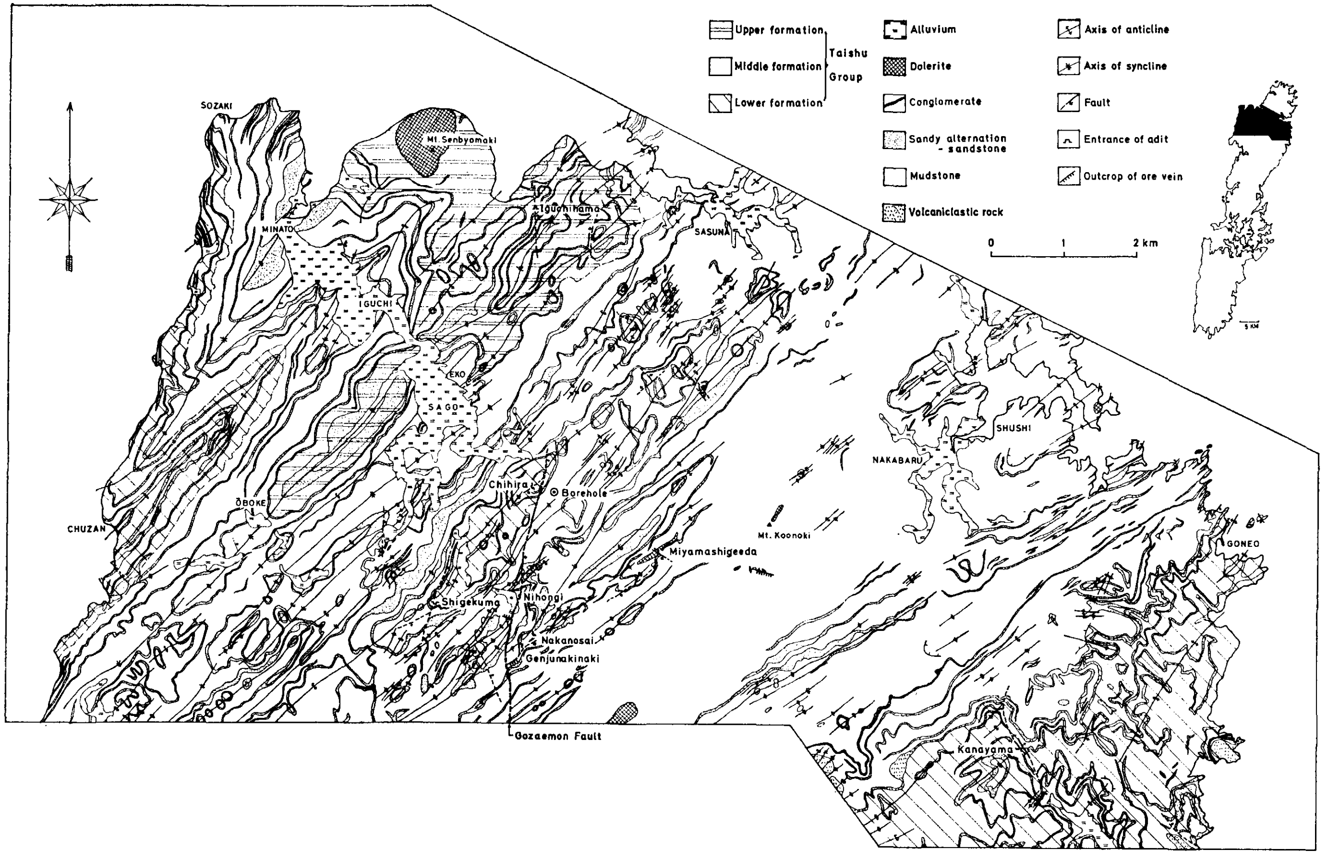


Fig. 5. Geologic map of Sago and Kin areas, Kamishima (modified after MITI, 1971).

Kamishima whose veins are less than 30 cm in width.

The lithofacies map around Sago and Kin areas is shown in Fig. 5. It is important that no acidic igneous rock crops out in the vicinity of the deposits.

It is obvious in Table 3 that all the deposits are characterized by the mineral association of sphalerite, galena, Fe-carbonate mineral and quartz. They essentially lack pyrrhotite and calcite. Shigekuma and Nihongi deposits yielded abundant silver minerals composed of tetrahedrite, and very fine grained nickel mineral, ullmannite in addition to the common mineral assemblage. Limonite and cerussite, which are found in some closed deposits and outcrops, can be concluded to be products of supergene alteration from their modes of occurrence.

The geological structure of Kamishima suggests that the distribution of almost all the deposits in Kamishima is limited around N-S fault or Gozaemon Fault, and NW faults (Fig. 5). Thus, the borehole prospecting was performed to the depth of 1,300 m through the Lower Formation, at the place near the Chihira deposit in Sago area (Fig. 5) by the Metal Mining Agency of Japan (MITI, 1974). Although lead-zinc ores were found in small amounts as veinlets in fractures along N-S fault, a lot of carbonate-quartz veinlets occurred through the cores. The chemical compositions of carbonate minerals have been investigated with a result of interest concerning ankeritization as described later.

3. *Ore deposits in Shimojima*

In Shimojima, metalliferous ore deposits are distributed in five areas: Ohfunakoshi, Izuhara, Sasu, Tsutsu, and Yora areas. They appear intimately with the 12-million-year-old biotite granite. Izuhara and Tsutsu areas occupy the peripheral part of the hornfels zone (Fig. 6).

*Ohfunakoshi area*: This area lies around the crest of anticline, and also on the gentle dipping or nearly horizontal bed of the Middle to Upper Formations of the Taishu Group. In the area, the presence of small granitic body is inferred in the shallow portion, as described afore. Recently, the borehole prospecting was carried out at Konjobana, and revealed that biotite hornfels appeared in the fine alternation of sandstone and shale at the depth of −150 m under the ground (MITI, 1975). Thus the presence of a cryptomass of granite seems reliable. Ore deposits in the area are subdivided into four veingroups: Ohfunakoshi, Konjobana, Ogata, and Misaki. They are impregnated along fractures trending N20°–40°W, and partly along ones trending N65°–85°W, as shown in Fig. 6. They yield abundant quartz and pyrrhotite ores with some sulfide minerals. The vein system and constituent minerals are listed in Table 4. The vein generally takes less than 1 m in width, but locally a barren quartz vein attains 7 m in width with remarkable comb structure.

At the outcrops of the veins, supergene alteration is so strong that such secondary minerals as limonite, melnikovite, marcasite, cerussite, and covellite-like minerals are commonly observed.

*Izuhara area*: Ore deposits in Izuhara area are principally narrow and short veins, filling fissures in plagiophyre and biotite hornfels. The vein system of the deposits generally shows the trend of NW, but the mineral assembalges are rather distinct from one another (Table 5). From the Nariaisai deposit,

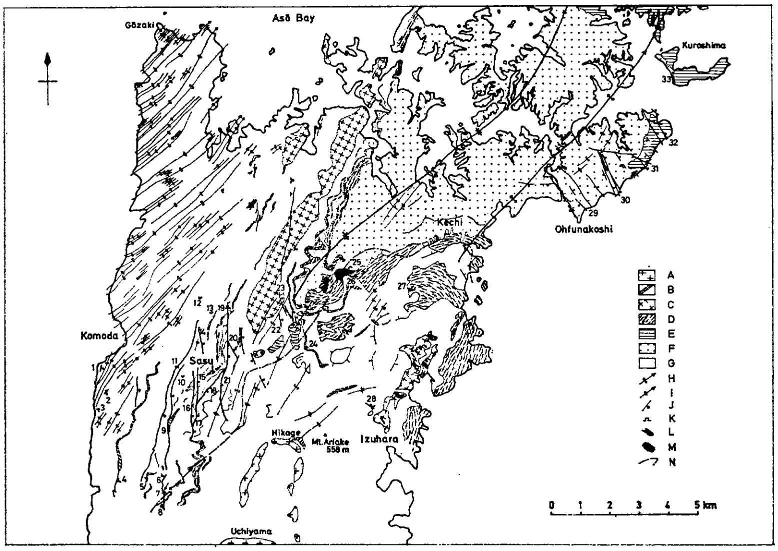


Fig. 6. Geologic map of the northern part of Shimojima, including Sasu, Izuhara, and Ohfunakoshi areas.
A: biotite granite, B: dolerite, C: quartz porphyry, D: plagiophyre, E: Upper Formation, F: Middle Formation, G: Lower Formation, H: anticline, I: syncline, J: fault, K: adit, L: pottery stone deposit, M: the place rich in pyrrhotite dissemination, N: outer boundary of hornfels zone. *Ore deposit* 1, 2, 3: Shiine, 4: Amanohara, 5: Shimoken, 6: Motoyamamichi, 7: Furukawa, 8: Kune-Toobu, 9: Akushidani, 10: Kunoe, 11: Urakochi, 12: Aré-Somen, 13: Nishikura, 14: Tsurue, 15: Misoge, 16: Yasuda-Taisho, 17: Showa, 18: Sennin-mabu-Somen, 19: Taihei, 20: Himi, 21: Shintomi, 22: Shiratake, 23: Maetake, 24: Misumiyama-Higashi, 25: Momijiyama, 26: Momiji-yama outcrop, 27: Kamisaka, 28: Nariaisai, 29: Ohfunakoshi, 30: Konjobana, 31: Ogata, 32: Misaki, 33: Kuroshima old adit.

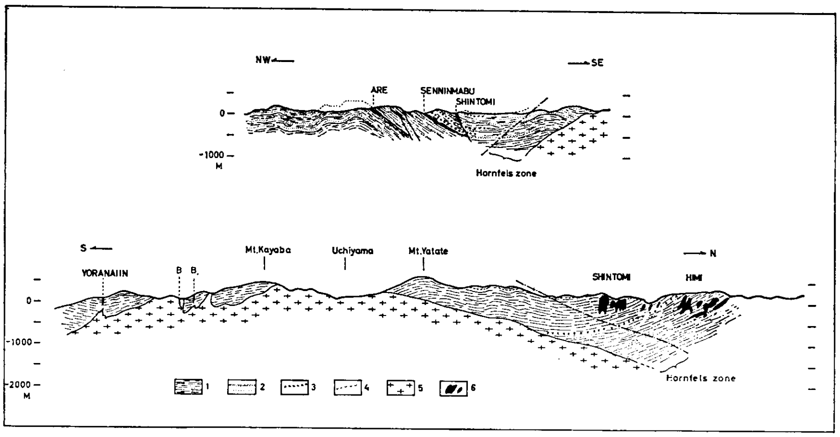


Fig. 7. Geologic sections of Shimojima.
1: mudstone, 2: sandstone, 3: quartz porphyry, 4: plagiophyre, 5: biotite granite, 6: ore body, B: tourmaline vein.

Table 4. Ore deposits in Ohfunakoshi area

| Ore deposit | Vein system | Constituent mineral | Adit & outcrop |
|---|---|---|---|
| Ohfunakoshi | N30-40°W, 80°S<br>N80°W, 90° | Po, Q, (Sph, Gn, Asp, Cer). | 3 old adits, 20 outcrops |
| Konjobana | N20-30°W, 80°N or S | Po, Q, (Asp, Cp, Py, Mac. Sph, Gn), Cc. | 18 outcrop |
| Ogata | N30°W, 80°N or S | Po, (Asp, Cp, Py, Mac, Sph, Gn, Bi) | 3 old adits, 18 outcrops |
| Misaki | N20-30°W, 65°E<br>N65°W, 60°N | Q, Po, (Cp, Mac, Py, Sph, Gn). | 12 outcrops |

Abbreviation: Po: pyrrhotite, Q: quartz, Sph: sphalerie, Gn: galena, Asp: arsenopyrite, Cer: cerussite, Cp: chalcopyrite, Py: pyrite, Mac: marcasite, Cc: calcite, Bi: native bismuth.

Table 5. Ore deposis in Izuhara area

| Ore deposit | Vein system | Constituent mineral | Adit & outcrop |
|---|---|---|---|
| Momijiyama | N55°W, 80°S<br>N72°W, 62°N | Po, Asp, Py, Tom, Q, (Sph, Gn, Cp) | Outcrop (1.5m in width) |
| Kamisaka | N55°W, 85°S | Cer, Gn, Sph. | 5 old adits |
| Nariaisai | N42°W, 85°N | Sph, Gn. Q, (Cer, Mim, Ang, Pym, Wul, Ant) | 3 old adits |

Abbreviation: Po: pyrrhotite, Asp: arsenopyrite, Py: pyrite, Tom: tourmaline, Q: quartz, Sph: sphalerite, Gn: galena, Cp: chalcopyrite, Cer: cerussite, Mim: mimetite, Ang: anglesite, Pym: pyromorphite, Wul: wulfenite, Ant: anatase.

sphalerite, galena, and some secondary minerals as cerussite, mimetite, anglesite, pyromorphite, and wulfenite are reported (OKAMOTO, 1953, 1958; SAKURAI, 1957). Anatase crystals are also described from the silicified palgiophyre of the deposit (MINATO and OKAMOTO, 1957). It is noteworthy that wulfenite occurs as a molybdenum-bearing mineral, which has never been found in other deposits except an occurrence of a small molybdenite in biotite granite at Hikage.

*Sasu (Taishu mine) area*: It is well known that many large ore deposits are distributed in Sasu area (MITI, 1974). Their vein systems and constituent minerals are listed in Table 6. There are three types of veins: N-S, NE or bedding-plane, and NW veins. The N-S veins are found along the left handed strike-slip faults, and are represented by Kunoe and Akushidani deposits in the western part; Tsurue, Misoge, and Yasuda-Taisho in the central; and Himi, Shintomi (or Okutomi), and Shiratake in the eastern part as shown in Fig. 8 (SASAKURA and UEHARA, 1958; UEHARA, 1959a, b, 1964; UEHARA and MATSUHASHI, 1961). The NE or bedding-plane veins are found along the bedding-plane faults trending generally N35°E, which are reverse faults developed in the boundary between sandstone or sandy alternation as foot wall and mudstone as hanging wall (MATSUHASHI, 1967, 1968). Aré-Somen, Urakochi-Somen, Tsurue-Somen, and Senninmabu-Somen deposits are representative (Fig. 8). It is remarkable that the Senninmabu-Somen deposit attains 2.2 km in the direction of the strike, and more than 800 m along the dip side. The NW veins, such

Table 6. Ore deposits in Sasu area

| | Ore deposit | Vein system | Length | Width | Constituent mineral |
|---|---|---|---|---|---|
| WESTERN | Shiine (or Unose) | N20°E, 40°E | 10 m | 0.05 m | Sph, Gn. |
| | Amanohara | N14°E, 63°E | 50 | 0.6 | Sph, Gn, Po, Q, Cc, Cp. |
| | Shimoken | N15°E, 60°E | 30 | 1.0 | Sph, Gn, Po, Cp, Q, Cc. |
| | Urakochi-Somen | N34°E, 36°E | 580 | 0.9 | Cc, Sph, Po, Gn, (Cp). |
| | Kunoe | N10°E, 56°E | 90 | 1.2 | Sph, Gn, Po, Cc. |
| | Kunoe-Somen | N37°E, 34°E | 190 | 0.8 | Sph, Po, Gn, (Asp, Cp, Q) |
| | Akushidani | N6°E, 57°E | 500 | 1.8 | Po, Sph, Gn, Asp, (Q, Cp) |
| | Akushidani-Uwaban | N6°E, 68°E | 110 | 5.8 | Sph, Gn, Po, Cc. |
| | Motoyamamichi | N15°E, 66°E | 8 | 0.7 | Asp, Q, (Po, Cp) |
| | Furukawa | NS, 60°E | 10 | 0.4 | Q, Asp, (Po, Co). |
| CENTRAL | Aré-Somen | N37°E, 53°E | 40 | 1.8 | Gn, Cp, Sph, Po, (Py, Q, Sid, Ank). |
| | Tsurue | NS, 66°E | 40 | 1.4 | Cc, Sph, Gn. |
| | Tsurue-Somen | N35°E, 36°E | 45 | 0.7 | Cc, Sph, Gn, (Po). |
| | Senninmabu-Somen | N34°E, 34°E | 2200 | 1.0 | Sph, Gn, Po, Cc. |
| | Misoge | N6°W, 64°E | 390 | 1.2 | Sph, Po, (Gn, Q) |
| | Yasuda-Taisho | NS, 57°E | 720 | 1.6 | Sph, Po, Asp, Q, (Gn, Cp). |
| | Showa | N33°E, 46°E | 150 | 0.9 | Sph, Po, (Gn, Cc). |
| EASTERN | Nishikura | N45°E, 40°E | — | — | Gn, Sph, Cc. |
| | Himi | NS, 62°E | 800 | 1.5 | Sph, Gn, Po, Cc. |
| | Himi-No. 1 Uwaban | N30°W, 64°E | 130 | 1.3 | Cc, Sph, Gn, (Po). |
| | Himi-No. 2 Uwaban | N10°W, 80°E | 210 | 1.2 | Cc, Sph, Gn, (Po). |
| | Shintomi | N5°E, 57°E | 740 | 1.2 | Sph, Gn, Po, Cc, Q, (Asp, Cp). |
| | Shintomi-Somen | N36°E, 35°E | 30 | 0.4 | Sph, Gn, Po. |
| | Shiratake | N8°W, 60°E | 25 | 0.5 | Sph, Gn, Cc. |
| | Shiratake Uwaban | N12°W, 73°E | 135 | 0.3 | Cc, Gn, Sph, Po, Q, (Asp). |

as Himi Nos. 1 and 2 Uwaban deposits, are locally found in the area. They are characterized by an abundant occurrence of calcite in addition to lead-zinc ores (MITI, 1974).

Ore deposits in the area show remarkable zoning or regular distribution of ore-forming minerals. Namely, each ore deposit or an ore body shows vertical zoning from lower to upper horizons as follows: quartz zone, pyrrhotite zone, sphalerite-galena zone, and calcite zone (UEHARA, 1964; MATSUHASHI, 1967). Furthermore, horizontal zoning or district zoning can be recognized in the area (MITI, 1974) as shown in Fig. 8: there are inner pyrrhotite zone and outer sphalerite-galena zone around biotite granite. The boundary line depicted by the assay map runs nearly parallel to the distribution of hornfels zone, which is developed just around biotite granite.

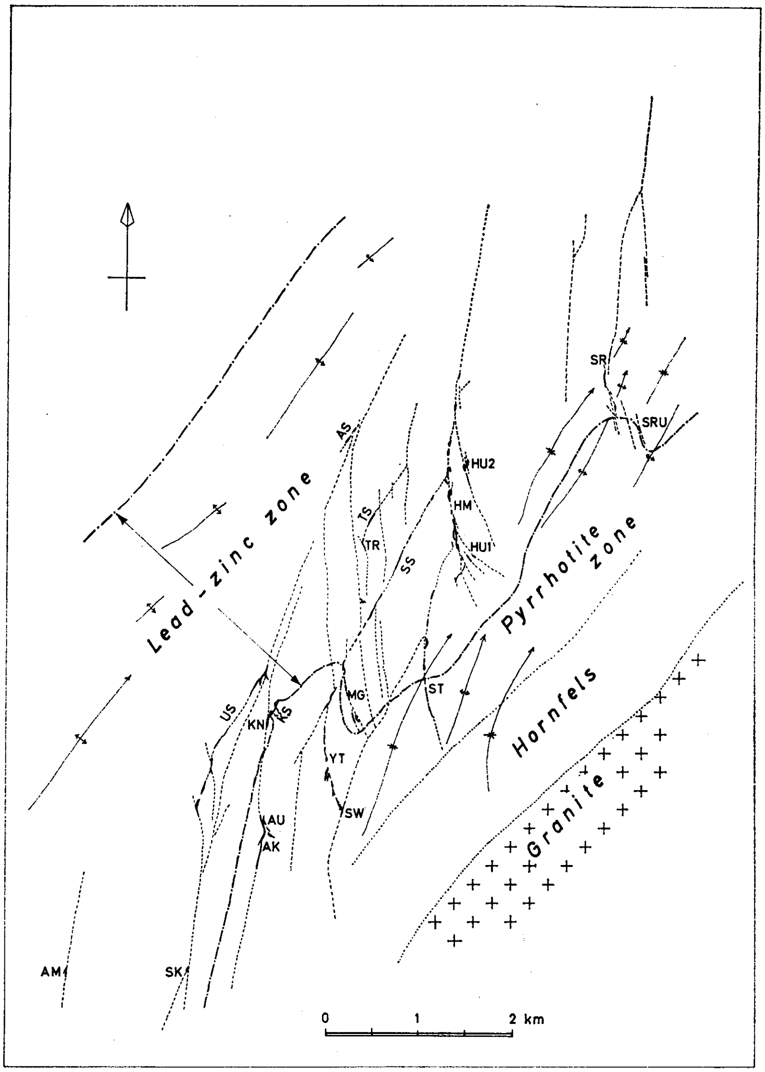


Fig. 8. Vein map of Sasu area on the horizon of 90 m under the sea level (MITI, 1974). AM: Amanohara, SK: Shimoken, US: Urakochi-Somen, KN: Kunoe, KS: Kunoe-Somen, AK: Akushidani, AU: Akushidani-Uwaban, AS: Aré-Somen, TS: Tsurue-Somen, TR: Tsurue, SS: Sennin-mabu-Somen, MG: Misoge, YT: Yasuda-Taisho, SW: Showa, HM: Himi, HU1: Himi No. 1 Uwaban, HU2: Himi No. 2 Uwaban, ST: Shintomi, SR: Shiratake, SRU: Shiratake Uwaban.

Concering the formation temperature of ores, fluid inclusions in quartz were investigated by MIYAZAWA (1961), TAKENOUCHI (1962), and IMAI *et al.* (1971), and sulfur isotopic fractionation was studied by TATSUMI (1965) and KIYOSU (1973). Minerals from the mine were also described by NISHIWAKI and SHIOBARA (1948), OKAMOTO (1958), and SHIROZU (1960, 1963).

*Tsutsu and Yora areas*: Ozakiyama deposit is an important lead-zinc vein in Tsutsu area. It consists of narrow veins along faults of NW and N-S. The

Table 7. Ore deposits in Tsutsu and Yora areas

| Area | Ore deposit | Vein system | Constituent mineral | Remarks |
|---|---|---|---|---|
| Tsutsu | Ozakiyama | N18°W, 55°E | calcite, sphalerite, galena. | 3 old adits |
| | Tsutsu | N45°W, 80°S | quartz, tourmaline. | 1 outcrop |
| Yora | Yoranaiin | N50°W, 70°E? | tellurobismuthite, tetradymite, cobaltite, tourmaline, chlorite, apatite, muscovite. | boulder |

host rock is composed of mudstone intercalating thin sandstone, which shows the strike of N10°E and the dip of 35°E. At the south coast of Tsutsu, several quartz-tourmaline veins are found in quartz porphyry, but they accompany no metalliferous minerals. They trend in the direction of NW and are characterized by comb structure of quartz crystals.

Yoranaiin deposit in Yora area, which is situated at the southeastern end of Shimojima, seems to be formed along NW faults developed in hornfels. The outcrop has not yet been found except veins in several boulders attaining about 3 m in diameter (MUTA, 1957c). The veins form networks of 5 to 10 cm in width, intersecting across the bedding plane of sandstone and shale. They are regarded as greisen-like veins, composed of tourmaline, chlorite, apatite, quartz, amethist, and muscovite. Cobaltite, tellurobismuthite, and tetradymite were found in close association with tourmaline and chlorite (SHIMADA, 1973b).

The outline of ore deposits or outcrops in the two areas is listed in Table 7.

## C. Geological aspects for localization of ore deposits

Because all metalliferous ore deposits of Tsushima are essentially impregnated in the fissures along faults, it should be noted that the ore deposits are controlled definitely by faults and fractures in the host rocks. There are two types of ore deposits; one is impregnated in fractures trending toward both N-S and NE, and the other is chiefly NW fractures. The former type is common in almost all the deposits in four areas, namely Sago, Nita-Miné, Sasu, and Tsutsu areas. The latter type is found in the deposits of the other four areas: Kin, Ohfunakoshi, Izuhara, and Yora areas. It is notable that the former four areas are distributed in the western part of the Tsushima Islands, and the latter four areas in the eastern part. Marked difference of the vein patterns between the eastern and the western parts is stereographically shown in Fig. 9.

In the western part of Tsushima, a dense distribution of the second order folds is recognized. Namely, in Kamishima, the second order folding structure is well developed in Sago and Nita areas, having the wavelength within several hundred meters. Ore deposits are concentrated around some N-S faults, such as Gozaemon Fault (Fig. 5). In Shimojima, the second order folding structure is strongly expressed around the coast of Komoda and the western part of Sasu area. However, the ore deposits in this part are not so large in scale as those in Kamishima. A lot of larger deposits are found in the east of the closely

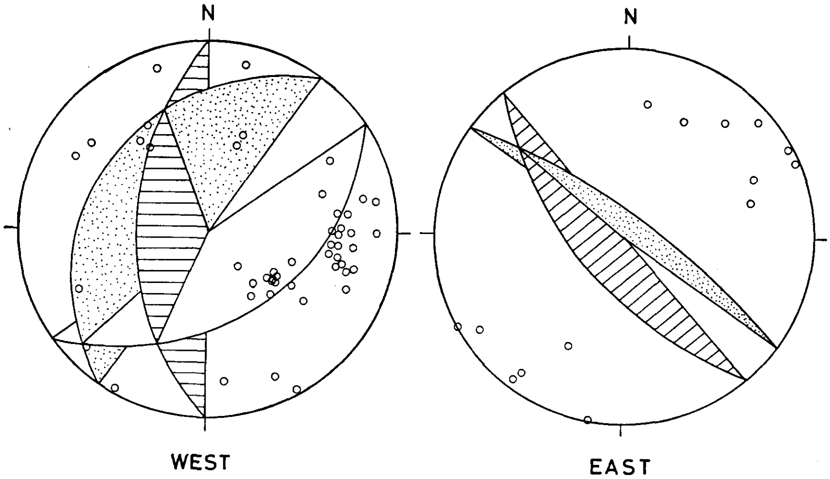


Fig. 9. Diagram showing the difference of vein patterns between the eastern part and the western part of Tsushima. The pole of the vein (small circle) and the the representative vein plans are plotted on Schmidt net (upper hemisphere).

folded area, which is the simple monoclinal part of the first order folding structure.

In the eastern part of Tsushima, the second order folding structure and faults trending N-S and NW are rather scarce, but the fractures trending NW are well developed. For instance, the dominant joints trend towards northwest, ranging from N25°W to N50°W, in Mitsushima town, the northern part of Shimojima (KITAMURA, 1962). In quartz porphyry and the neighbouring sediments at Izuhara town, the trend of fissures is statistically the strike of N40°W with nearly vertical dip (SUZAKI *et al.*, 1970). As mentioned above, NW veins are extremely concentrated in the Ohfunakoshi area.

Difference of fracture patterns and vein systems between the eastern and the western parts of Tsushima are considered to be definitely affected by the difference of geological structures, especially folding features, which are also related to the formation of "Korea Strait Tectonic Line" (MURAUCHI, 1972; TOMITA *et al.*, 1975), provincially named here "Off Nita Fault" and "Off Komoda Fault" (Fig. 4). When the tectonic movement arose through the "Taishu basin", horizontal compressive forces might acted along northwest-southeast lines. Both Off Nita and Off Komoda Faults might be regarded as ruptures due to a horizontal couple derived from the main horizontal compression. Minor folds and shear fractures in the eastern part is considered to have resulted from horizontal movement along such vertical faults as Off Nita and Off Komoda Faults.

It is observed that the nature of fractures varies with competencies of host rocks. In Sasu area of Shimojima, bedding-plane faults are found only in the horizon, where thin sandstone bed is dominantly intercalated. Where the sandstone bed pinches out, the fault dies out. Thereby, the distribution of bedding-plane vein is limited to the area in which sandstone beds are developed

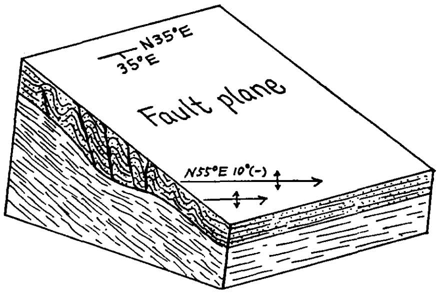


Fig. 10. Sandstone bed in Sasu area, showing interfolding due to slump structure. Bedding-plane reverse fault preferentially formed on the hanging wall side of the sandstone bed.

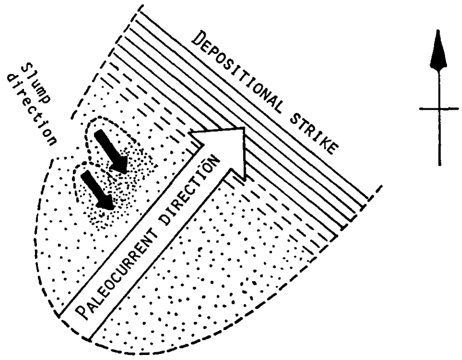


Fig. 11. Schematic diagram showing the directions of slump movement and main paleocurrent during the deposition of the " Taishu basin ".

(MATSUHASHI, 1968). Development of NE veins in Sago area, Kamishima, also shows the same relation of fracturing controlled by lithofacies, as described later.

At galleries in the Taishu mine and also at outcrops of the Taishu Group, slump structures in sedimentary rocks are frequently observed, taking such as hook-shaped overfolds of sandstone slabs, and interstrata isoclinal folds or drag like ones, especially in the horizons of the Senninmabu and the Urakochi sandstone beds. The axes of the folds trend towards N40°–70°E, and their axial planes dip southwestwards. If these evidences are applied to gravity-generated movement of small lateral displacement during the sedimentation of the Taishu group, it presumably seems that slump movement occurred in the direction of NW to SE (Figs. 10 and 11). Meanwhile, the direction of paleocurrent on the Taishu Group was indicated to be northeastwards by various sedimentary structures (NAGAHAMA, 1967; OKADA *et al.*, 1971). However, some ripple marks frequently show the direction of paleocurrent to be southeastwards, as shown in Fig. 12. This trend corresponds well to that of the slump movement above mentioned.

This opinion is quite distinct from that of MATSUHASHI (1968). MATSUHASHI suggested that the complicated folding-like structure in sandstone beneath the bedding-plane fault was a drag fold, which had been formed by the movement of the reverse fault. This seems conflicting, because sandstone is more competent than mudstone and shale and the drag-like folds can be observed even along the weak bedding-plane fault. Therefore, it is concluded that reverse bedding-plane faults were formed particularly along sandstone beds having abundant slump structure to form consequently open fractures adequate for localization of ores.

A more important fact pertinent to the formation of fractures and ore-localization is that when a N-S sheared fault cuts across the sandstone bed or

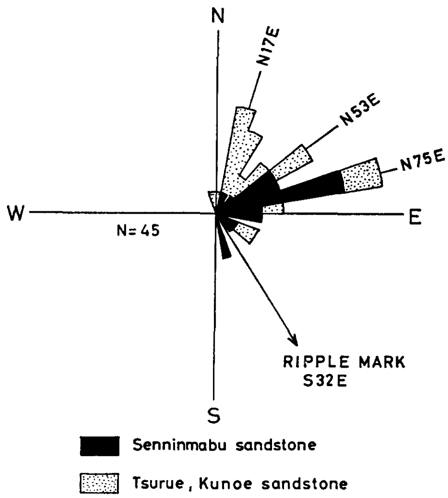


Fig. 12. Paleocurrent directions measured from sole marks on the sandstone in Sasu area. Each direction is restored to the initial horizontal state. Depicted from the data after TAKAHASHI and MATSUHASHI (1970).

igneous dike, many dispersed faults and fractures are observed in these competent rocks, though a simple fault is formed within mudstone and shale. The deposits in Nita-Miné area, such as Miné-Kanayama, are considered to be typical. In Sasu area, some bonanzas of so-called "Hangan-Kotai" or Porphyry Ore Body in the Himi and Akushidani deposits occur in such structural sites.

## III. Shigekuma-type ore deposits

### A. General statement

As described in II.B.2., ore deposits in Kamishima show rather common mineral assemblage, which are distinct from those of ore deposits in Shimojima. In this paper, ore deposits in Kamishima are provisionally named "Shigekuma-type", and those in Shimojima "Taishu-type".

The purpose of this chapter is to describe geological features, constituent minerals, and some characteristics of mineralizations and ore localization in the ore deposits of Shigekuma and Nihongi, which are representative Shigekuma-type deposits.

Shigekuma and Nihongi deposits in Sago area are essentially narrow fissure filling veins, which consist of silver-lead-zinc ores. They lie under some old adits near the surface.

At the Shigekuma deposit, the production recorded in March, 1971 was 1,600 metric tons per month for raw ores, and their grade attained 2% of lead, 3% of zinc, 0.07% of copper, and 200 gram/ton of silver. The grade of massive silver ore was sometimes 3,000 to 5,000 gram/ton.

The Nihongi deposit is situated about one kilometer east of the Shigekuma

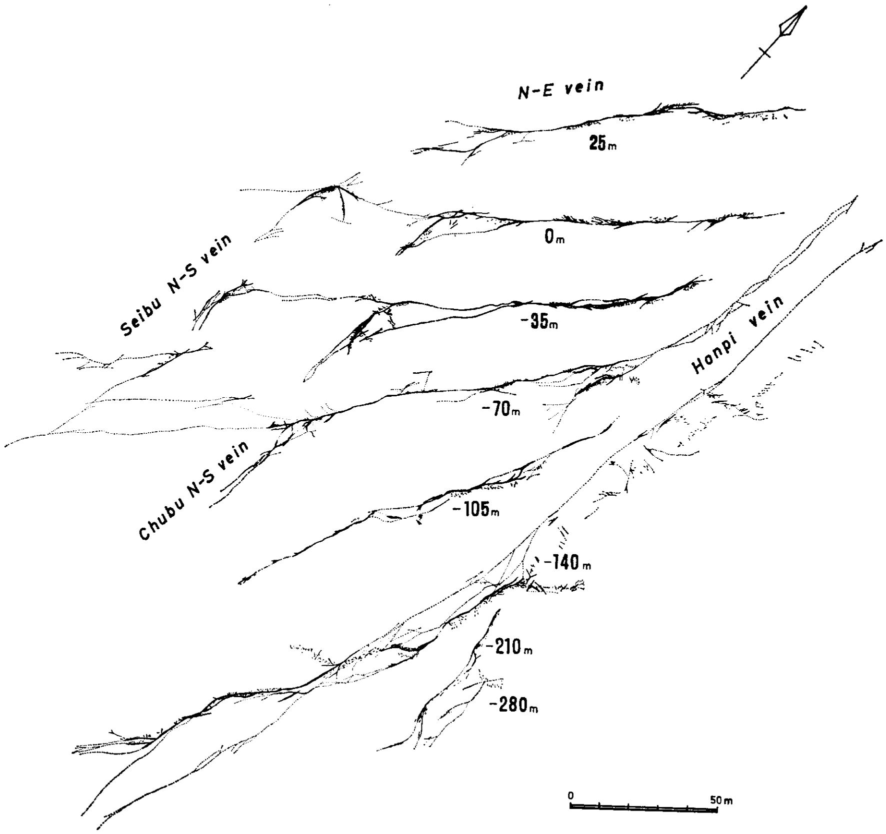


Fig. 13. Vein map of the Shigekuma deposit.

deposit (Fig. 5). Raw ores were produced in 400 tons/month at that time, and they contained 3% of zinc, 0.1% of lead, and 50 gram/ton of silver.

## B. Structural control

### 1. *Shigekuma deposit*

The Shigekuma deposit was mined chiefly in eight levels from +25 m to −280 m. It is interesting that the vein vanishes admirably at the deepest level. Fig. 13 is the plan of eight levels showing detailed features of the veins. It can be seen in the figure that ore localization is controlled by two kinds of faults, namely NE and N-S trending faults. Thus the ore veins are familiarly called Shigekuma NE Vein, Seibu N-S Vein, Chubu N-S Vein, and Shigekuma Honpi Vein.

Four NE faults are observed in the deposit. They are dip-slip or reverse faults with sheared zone of 1 m or less in width. The direction of the net slip was recognized with slickenside to be northwestwards (Fig. 14). Mineralization was found abundantly in the NE faults between mudstone of hanging wall and sandy alternation of foot wall. The NE fault runs almost comformably with

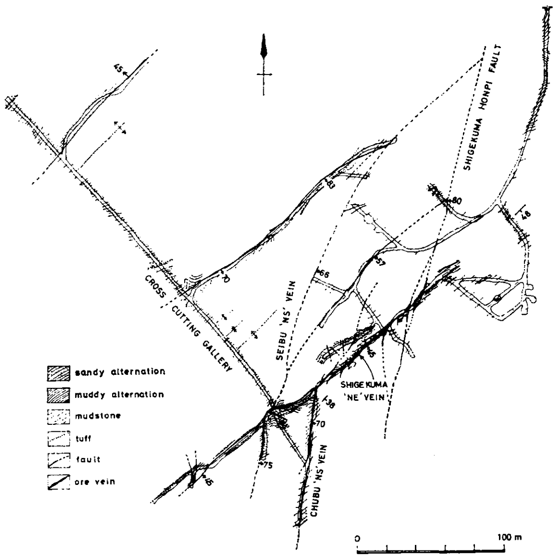


Fig. 14. Geology on the 0 m level of the Shigekuma deposit (modified after FUKUMOTO, K.).

the bedding-plane, but it intersects the strata around the crest of the fold near the surface of the earth.

The N-S fault is a left handed strike-slip fault. The host rock, especially mudstone, is pulverized to fine grained gouge having 1 to 3 m in width along the Shigekuma Honpi Fault. It strikes N10°E and dips 80°E.

Besides two kinds of faults, NW trending fissures are abundant in sandy alternation along sheared faults, and are frequently filled with ores to form short branch veins.

### 2. *Nihongi deposit*

At the Nihongi deposit, exploitation was taken in three levels: 0 m, −70 m, and −140 m levels. As shown in Fig. 15, the geological structure of the deposit displays more complicated features than that of Shigekuma, because many minor folds and multiple dislocation are recognized. Faults are characteristically developed in sandstone bed and sandy alternation parts. Ore veins are obviously controlled by N-S, E-W, and NW faults. The former two faults, represented by the Honpi Vein, Gozaemon Fault, and Uwaban Vein, are associated with markedly sheared zone. The last one is limited among N-S faults, and accompanies no sheared zone, as observed in the Shitaban Vein and several minor ones.

### 3. *Stress analysis*

The directions of slip along faults indicate two representative faults of N-S dipping 80°E and N80°W dipping 75°E to be conjugate. The stress distribution obtained from the set using GZOVSKII's method shows that the axis of maximum principal stress $\sigma_1$ has the direction of N41°W, being nearly horizontal. $\sigma_3$ is parallel to a bedding-plane or folding axis (Fig. 16). WATANABE, Y. (1972MS)

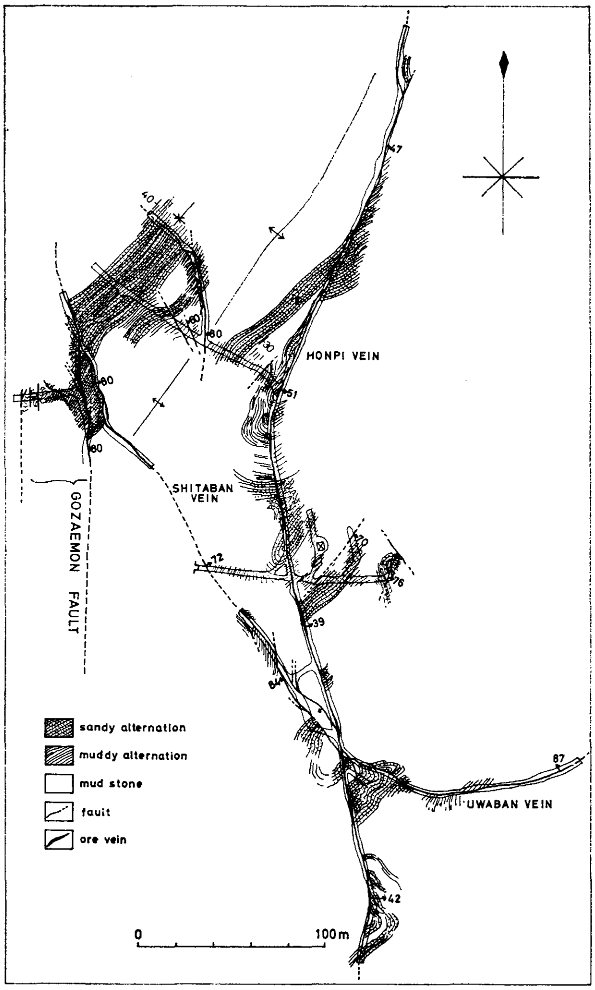


Fig. 15. Geological map on 0 m level of the Nihongi deposit (modified after FUKUMOTO, K.).

measured the distribution of joints filled with segregated quartz, which are developed in sandstone in Sago area, and showed that the most dominant joints trend towards N45°W, dipping 70°–80°NE, as shown in Fig. 16. In this area, therefore, the direction of maximum principal stress well coincides with that of the most dominant joints, and also with that of branch veins, which correspond to tension fractures.

From these results, it is concluded that horizontal compressive forces trending northwest deformed the strata, and formed the N-S and N80°W trending sheared faults and the NW trending tension fractures. The NE faults with various dip angles may be considered tension fractures due to release of stress, which have turned to be reverse sheared faults by a series of compression at the tectonic movement.

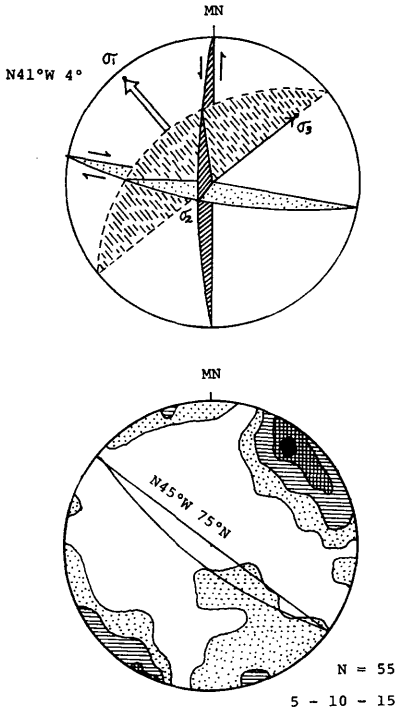


Fig. 16. Top: Stress field analysis in Sago area, using GZOVSKII's method (upper hemisphere). Bottom: Frequency of joints filled with segregated quartz vein in Sago area (after WATANABE, Y., 1972MS).

## C. Mineral sequence

### 1. *General character*

There are some distinguishing characters of the ore and gangue minerals. The mineral assemblages of ores are almost the same throughout the veins, and do not vary with depth. From top to bottom, neither rhythmic banding structure nor comb one is observed. Generally, the ore contains a lot of gangue stones, namely breccias of such host rocks as mudstone, sandstone, and their alternation. Sphalerite, which is the most abundant and important ore mineral, is always of a pale brown color.

### 2. *Mineral sequence*

The sequence of mineral deposition is best explained by dividing the mineralization into four stages on the basis of crustification and intersecting.

*Stage I.* The initial stage of formation of the veins is generally represented by sphalerite, with small amounts of coarse galena, ullmannite, and siderite. Siderite occurs locally as a thin band along the vein-wall (Fig. 17). It may be segregation product from host rocks, since some mudstones of the Taishu Group contain siderite as detected by an x-ray diffraction analysis. Sphalerite

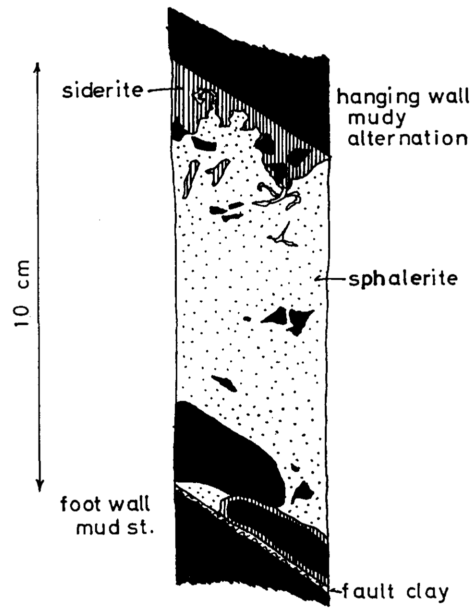


Fig. 17. Sketch showing the mode of occurrence of siderite and sphalerite ores in the stage I. Locality: Spot 31, −70m level, Shigekuma deposit.

makes massive vein, and involves a small amounts of corroded relict of siderite. Small patches of coarse galena are found in and around sphalerite, and seem to have been formed somewhat later than sphalerite. Very fine grained ullmannite occurs as veinlets cutting sphalerite and siderite. Ullmannite occurs largely as a myrmekitic relict in the mineral assemblage of the next stage (SIHMADA and WATANABE, 1973).

*Stage II.* The end of the stage I is marked by deposition of tetrahedrite and chalcopyrite (Fig. 18). The two minerals commonly occur as an intimate association, and clearly intersect sphalerite ores and locally replace them. At their boundary, the concave surface of chalcopyrite develops into tetrahedrite. In some specimens, tetrahedrite is veined by chalcopyrite. Tetrahedrite is also observed as unsupported fragments in the veinlet of chalcopyrite. These sulfide minerals are locally followed and invaded by quartz veinlet. In this case, sericite and chlorite are formed between host rocks or gangue stones and quartz veinlets.

*Stage III.* This stage is characterized by an abundant occurrence of galena. The mineral is fine grained, and shows foliated or flow-like structure as if the relicts of the former stage minerals were transported and corroded by a solution (Fig. 19). Between tetrahedrite and galena, myrmekitic intergrowth of bournonite and sphalerite is formed. It seems to be a reaction rim considered from their chemical compositions.

*Stage IV.* This is the final stage composed of siderite, ankerite, and quartz. Siderite is predominant gangue mineral in the Seibu N-S Vein and NE Vein. The siderite is coarse and massive, but not banded. It is noteworthy that the

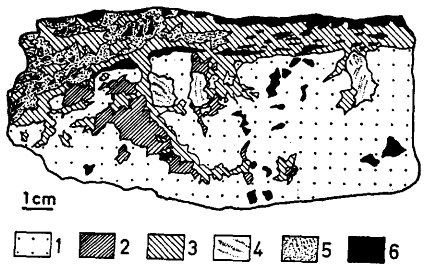


Fig. 18. Sketch of an ore, showing sphalerite-coarse galena (stage I) and tetrahedrite-chalcopyrite-quartz (stage II). 1: sphalerite, 2: tetrahedrite, 3: chalcopyrite, 4: coarse galena, 5: quartz, 6: mudstone fragment. Locality: −210 m level, Shigekuma.

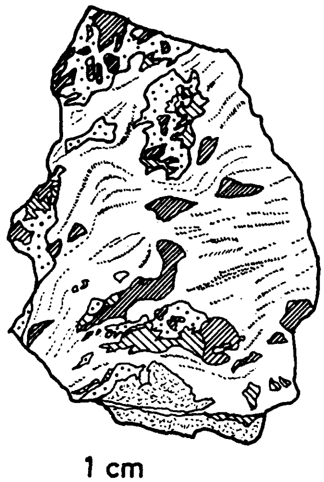


Fig. 19. Sketch showing the mode of occurrence of foliated galena (stage III) including relicts of the former products. The symbols are the same as those in Fig. 18. Locality: 0 m level, Shigekuma.

siderite vein contains a large amount of breccias of mudstone as well as mineral fragments of the former stages. Ankerite and quartz veins cut across sulfide minerals, but also occur markedly along fissures in the host rock.

3. *Summary of mineral sequence*

The principal stages of mineral deposition of silver-lead-zinc ores and gangue minerals were reasonably well established, and the mineral sequence of each stage was considerably defined. The sequence of the Shigekuma deposit is shown graphically in Fig. 20. Some details are excluded in the figure, but the complete sequence may be summarized as follows:

Stage I: Minor amount of siderite segregated from the host rock; abundant sphalerite next; coarse grained galena and small amounts of ullmannite overlapping and later than sphalerite.

Stage II: Tetrahedrite generally early; chalcopyrite just later, but mainly overlapping with tetrahedrite; minor quartz slightly later; sericite and chlorite overlapping with quartz.

Stage III: Principally galena; reaction rim of bournonite and sphalerite slightly early.

Stage IV: Deposition of siderite; ankerite and quartz nearly contemporaneous with siderite or just later.

The mineral sequence of the Nihongi deposit is very similar to that of Shigekuma (Fig. 21). However, much deposition of pyrite with quartz, called stage IB, is extremely characteristic, besides in Shigekuma where pyrite nodules

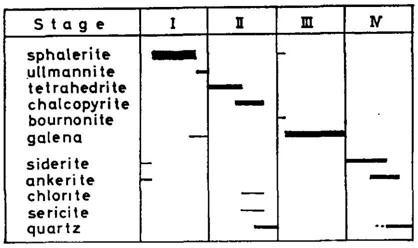


Fig. 20. Schematic diagram of mineral sequence in the shigekuma deposit.

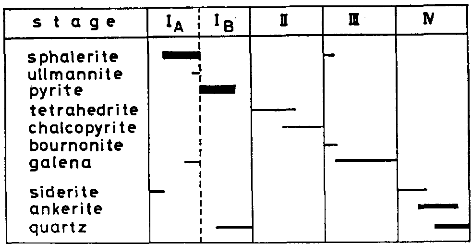


Fig. 21. Schematic diagram of mineral sequence in the Nihongi deposit.

and framboids in sedimentary origin are captured only as small relicits in chalcopyrite and other minerals.

## D. Mineral deposition and zonality

Fig. 22 indicates schematically the distribution of minerals of the stages I, II, and III. It is noteworthy in the figure that the distributive areas of the stage II and III are confined within the area of stage I. The ore shoot of each stage is different with one another. The minerals of the stage IV are, however, distributed over a wide area in and around the mineralized areas of stage I to III.

These facts suggest that the tectonic fracturing took place continuously from the time before the deposition of stage I to that just after the mineralization of stage III. The fracturing might have been growing and widening incessantly. Ore-forming solutions were supplied intermittently during the period, and the depositions were overlapped. Before the mineralization of stage IV, tectonic reopening took place in relatively wide area, then the deposition of stage IV followed.

This kind of mineralization related to tectonic causes can be regarded as a typical polyascendent zoning (KUTINA, 1965), and also as the first order, stage by stage zonality after SMIRNOV (1960). Furthermore, it is referred to "tectonic opening-type" rather than "repeated tectonic fractures-type" in subdivisions of the zonality in SMIRNOV's sense.

## E. Compositional variation of minerals

### 1. *Sphalerite*

Since KULLERUD (1953) presented the experimental curve that showed the iron content of sphalerite in equilibrium with both pyrite and pyrrhotite as a function of temperature, this sphalerite geothermometer has long been applied to many ore deposits and concurrently checked up by numerous investigators. At present, there are several conflicting versions of phase relations in the system Zn-Fe-S in the temperature below 500°C, although it is generally accepted that both sulfur fugacity and temperature strongly influence the composition of sphalerite. Therefore, chemical analyses of natural sphalerite may

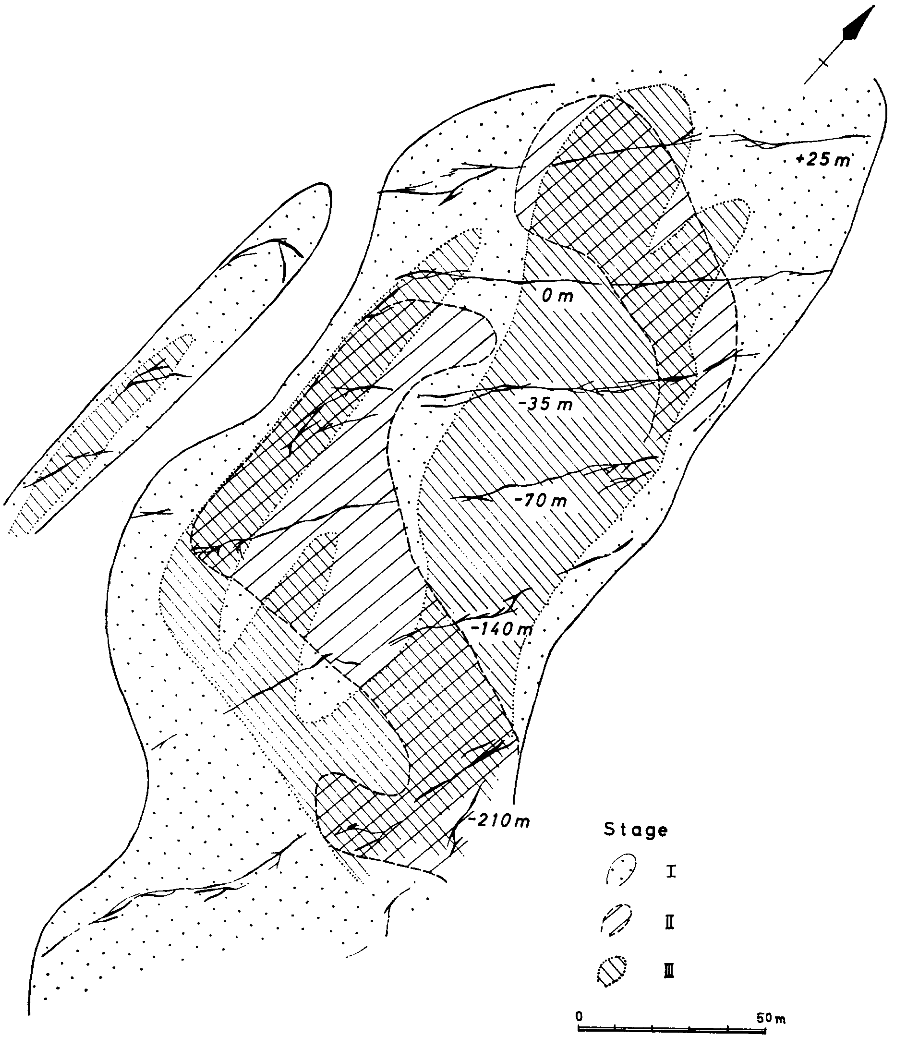


Fig. 22. A plan showing the spacial distribution of minerals of stages I, II, and III in the Shigekuma deposit.

now be needed to unravel the phase relations in the synthetic system rather than providing informations to thermometry of ore deposits.

Sphalerites in the deposits of Kamishima are normally light brown to slightly dark brown in color and associated with pyrite or siderite.

*a. Chemical composition of sphalerite*

X-ray diffraction techniques and electron probe microanalyses were used to determine the composition of sphalerites in ores of Sago and Kin areas, Kamishima.

*Unit cell edges*: Unit cell edges for twenty-seven sphalerites were measured by a JDX-5P x-ray diffractometer with internal standards of silicon and

Table 8. Unit cell edges and iron contents of sphalerites

| Sample No. | $a_0$(Å) | FeS mol% | Locality | | Sample No. | $a_0$(Å) | FeS mol% | Locality | |
|---|---|---|---|---|---|---|---|---|---|
| Ts-245 | 5.4110 | 1.2 | Shigekuma | 0m | Ts-371 | 5.4120 | 3.8* | Shigekuma | −140m |
| Ts-246 | 5.4104 | 1.6 -1.9 | | 0m | Ts-368 | 5.4114 | 2.7* | | −210m |
| Ts-248 | 5.4114 | 2.7* | | 0m | Ts-258 | 5.4102 | 0.5* | Nihongi | 0m |
| Ts-367 | 5.4125 | 4.8* | | −35m | Ts-381 | 5.4109 | 1.8* | | 0m |
| Ts-253 | 5.4112 | 2.1 -2.6 | | −35m | Ts-382 | 5.4120 | 3.8* | | −70m |
| Ts-254 | 5.4117 | 3.3* | | −35m | Ts-383 | 5.4115 | 2.9* | | −70m |
| Ts-255 | 5.4106 | 1.9 | | −35m | Ts-384 | 5.4114 | 2.7* | | −70m |
| Ts-361 | 5.4107 | 1.4* | | −35m | Ts-237 | 5.4141 | 7.9* | Kanayama | +10m |
| Ts-244 | 5.4105 | 1.3 -1.4 | | −70m | Ts-236 | 5.4149 | 9.5* | | 0m |
| Ts-250 | 5.4118 | 3.5* | | −70m | Ts-392 | 5.4166 | 13.1* | | 0m |
| Ts-252 | 5.4125 | 4.8* | | −70m | Ts-667 | 5.4149 | 9.5* | | 0m |
| Ts-375 | 5.4112 | 2.3* | | −105m | Ts-673 | 5.4167 | 13.4* | | 0m |
| Ts-757 | 5.4123 | 4.4* | | −140m | Ts-666 | 5.4149 | 9.5* | | −30m |
| Ts-317 | 5.4120 | 3.4 -3.6 | | −140m | | | | | |

* obtained from the equation shown in Fig. 23.

Table 9. Chemical compositions of sphalerites

| No. | Sample No. | Zn | Fe | S | $Total_{wt\%}$ | $ZnS_{mol\%}$ | $FeS_{mol\%}$ | Locality |
|---|---|---|---|---|---|---|---|---|
| 1 | Ts-253A | 66.0 | 1.5 | 32.6 | 100.1 | 97.4 | 2.6 | −70m, 26 spot |
| 2 | Ts-253B | 65.9 | 1.2 | 32.9 | 100.0 | 97.9 | 2.1 | |
| 3 | Ts-255A | 66.5 | 1.1 | 32.8 | 100.4 | 98.1 | 1.9 | −35m, 26 spot |
| 4 | Ts-255B | 66.6 | 1.1 | 32.8 | 100.5 | 98.1 | 1.9 | |
| 5 | Ts-257A | 67.1 | 0.8 | 32.5 | 100.4 | 98.6 | 1.4 | −140m, 24 spot |
| 6 | Ts-257B | 66.6 | 1.2 | 32.9 | 100.7 | 98.0 | 2.0 | |
| 7 | Ts-244A | 67.1 | 0.8 | 33.1 | 101.0 | 98.6 | 1.4 | −70m, 25 spot |
| 8 | Ts-244B | 67.0 | 0.8 | 33.5 | 101.3 | 98.7 | 1.3 | |
| 9 | Ts-245A | 66.7 | 0.7 | 33.2 | 100.6 | 98.8 | 1.2 | +15m, 25 spot |
| 10 | Ts-245B | 66.4 | 0.7 | 33.3 | 100.4 | 98.8 | 1.2 | |
| 11 | Ts-246A | 67.2 | 0.9 | 32.7 | 100.8 | 98.4 | 1.6 | +15m, 24 spot |
| 12 | Ts-246B | 66.7 | 1.1 | 32.8 | 100.6 | 98.1 | 1.9 | |
| 13 | Ts-317A | 63.1 | 1.9 | 34.9 | 99.9 | 96.6 | 3.4 | −140m, 20 spot |
| 14 | Ts-317B | 62.9 | 2.0 | 35.1 | 100.0 | 96.4 | 3.6 | |

Conditions of electron probe microanalyses: 20 kV, 0.02 micro A.
Standards: Pure metals of iron and zinc; Chalcopyrite.
Correction: Philibert's, and Poole and Thomas's methods.

fluorite. The analysis was taken three times on 1/4° per minute scans for the spacings of the $d(311)$, $d(331)$ and $d(422)$. The dimension of the unit cell edges ranges from 5.4104 to 5.4167 Å, as shown in Table 8.

*Electron microprobe analysis*: Fourteen sphalerites from Shigekuma were analyzed by a JXA-5A analyser with results shown in Table 9. The content of FeS ranges from 1.2 to 3.6 mol%, and the contents of manganese and cadmium are less than 0.1 wt%. The variation of iron content in a single grain or on a polished specimen was detected up to 0.6 FeS mol% in maximum.

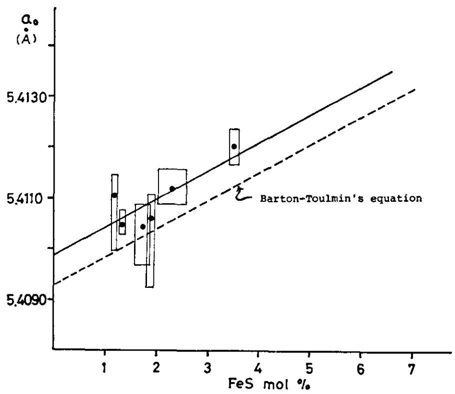


Fig. 23. Unit cell edge versus FeS mol% of sphalerites from Shigekuma.

*Correlation between unit cell edge and iron content*: Fig. 23 shows the relation of unit cell edges versus iron contents of sphalerite. An experimental equation obtained has 0.0006 Å higher value than that presented by BARTON and TOULMIN (1966).

Thus the chemical composition of sphalerite was also evaluated from the unit cell determination. From these (Table 8) it is concluded that the contents of FeS in sphalerites in Shigekuma, Nihongi, and Kanayama deposits range from 1.2 to 4.8 mol%, 0.5 to 3.5 mol%, and 9.5 to 13.4 mol% respectively.

*b. Compositional variations of sphalerite in Shigekuma*

Iron contents of sphalerites belonging to the stage II in Shigekuma were obtained as described above, and were plotted on Fig. 24. From the figure, it can be concluded that no conspicuous trend in variation of iron contents is recognized; in other words, sphalerite with varying chemical composition is distributed randomly throughout the deposit.

Iron-bearing minerals coexisting with sphalerite are commonly siderite of the stage I and very rarely pyrite nodule of the sedimentary origin. Compositional variation of sphalerite connected to mineral association was not observed.

2. *Ullmannite*

Ullmannite is a comparatively rare mineral, occurring in veins with siderite and nickel minerals as gersdorffite and niccolite (PALACHE *et al.*, 1944).

From the Shigekuma and Nihongi deposits, ullmannite was described by SHIMADA and WATANABE (1973). It was the second description of ullmannite in Japan. The mineral occurs mainly in tetrahedrite and chalcopyrite as fine grained relicts up to 40 microns across, and partly as a veinlet cutting sphalerite and siderite of the stage I. Although the mineral is a minor constituent in Shigekuma, it is rather widely found in the ores from upper to lower levels.

In reflected light, the mineral is white in color and isotropic. Its microhardness ranges from 453 to 515 kg/mm$^2$ with a load of 10 g.

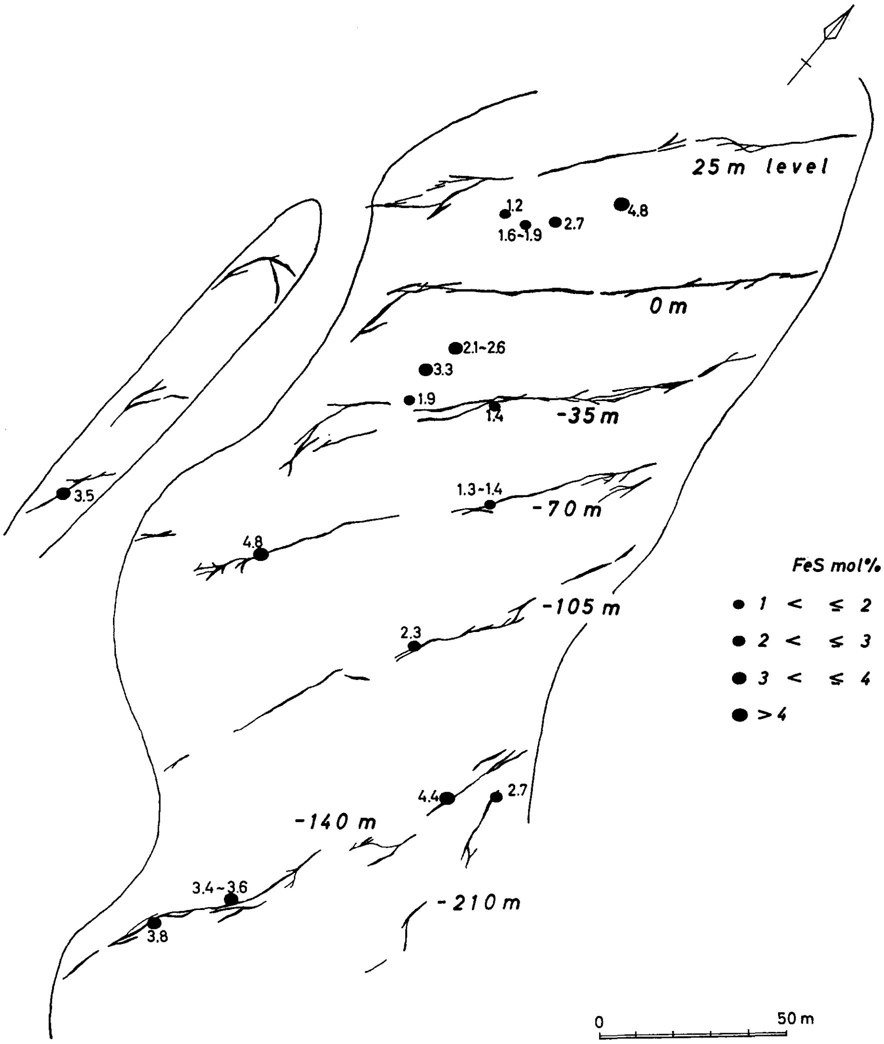


Fig. 24. Distribution of FeS mol% in sphalerites within the mineralization area of stage I (Shigekuma deposit).

*Chemical compositions of ullmannite*: Four ullmannite grains in various mineral assemblage were analyzed with an electron microprobe. The results are shown in Table 10. The mineral is generally known as a sulfide-antimonade of nickel, with small amounts of cobalt and iron substituting for nickel, and also arsenic and bismuth for antimony. Ullmannite from Shigekuma and Nihongi, however, is indicated to have chemical formula close to the ideal formula, NiSbS (Table 10).

3. *Tetrahedrite*

Numerous reports on the minerals of tetrahedrite-tennantite series have been presented from various kinds of ore deposits. In Japan, the mineral occurs

Table 10. Chemical compositions of ullmannites from Shigekuma

| Sample | Ni | Co | Fe | Zn | Sb | S | Total | Chemical formula |
|---|---|---|---|---|---|---|---|---|
| 1 | 25.9 | 0.9 | 0.1 | 0.3 | 58.1 | 14.6 | 99.6 | $(Ni_{0.95}Co_{0.03}Zn_{0.01})_{0.99}Sb_{1.03}S_{0.98}$ |
| 2 | 26.8 | 0.2 | 0.1 | 0.3 | 58.5 | 14.3 | 100.2 | $(Ni_{0.98}Co_{0.01}Zn_{0.01})_{1.00}Sb_{1.04}S_{0.96}$ |
| 3 | 26.2 | 0.8 | 0.5 | 0.2 | 57.8 | 15.0 | 100.5 | $(Ni_{0.94}Co_{0.03}Fe_{0.02}Zn_{0.01})Sb_{1.01}S_{0.88}$ |
| 4 | 26.2 | 0.5 | 0.6 | 0.2 | 58.3 | 14.6 | 100.4 | $(Ni_{0.96}Co_{0.02}Fe_{0.02}Zn_{0.01})Sb_{1.02}S_{0.97}$ |
| 5 | 27.6 | | | | 57.3 | 15.1 | 100.0 | NiSbS (ideal) |

1 and 2: occurred as relicts coexsisting with sphalerite,
3 and 4: relicts in chalcopyrite.

Table 11. Silver content in tetrahedrite, calculated from the value of unit cell edge

| sample No. | $a_0$(Å) | atm% | wt% | Locality |
|---|---|---|---|---|
| Ts-245 | 10.414 | 1.6 | 3.2 | Shigekuma 0m, 25 spot |
| Ts-248 | 10.460 | 5.2 | 9.6 | Shigekuma 0m, 23 spot |
| W8205A | 10.548 | 12.1 | 21.6 | Shigekuma −35m, 30 spot |
| W8205B | 10.524 | 10.2 | 18.3 | Shigekuma −35m, 30 spot |
| Ts-447 | 10.460 | 5.2 | 9.6 | Shigekuma −70m, 31 spot |
| Ts-375 | 10.538 | 11.3 | 20.2 | Shigekuma −105m, 27 spot |
| Ts-449 | 10.422 | 2.3 | 4.3 | Shigekuma −140m, 27 spot |
| W8306A | 10.556 | 12.7 | 22.6 | Shigekuma −210m, 27 spot |
| Ts-258 | 10.564 | 13.4 | 23.8 | Nihongi 0m, Honpi |
| Ts-381 | 10.436 | 3.4 | 6.2 | Nihongi 0m, Shitaban |

in pyrometasomatic deposits, veins, and also in the strata bound type deposits of Kuroko and Kieslager (KATAYAMA, 1934; SAKURAI and SUGIYA, 1934; HARADA and KITAHARA, 1952; WATANABE, 1943; ISHIBASHI, 1953; USHIZAWA, 1969; YUI, 1971).

Concerning argentian tetrahedrite, a high silver content of 20.1 wt% was reported from a gold-silver ore in the Takatama mine, Fukushima Prefecture (NISHIWAKI *et al.*, 1971). In Kuroko deposits, tetrahedrite contains 4.7 to 10.7 wt% silver (YAMAOKA, 1969; YUI, 1971). PETRUK and staff (1971) reported tetrahedrite with silver up to 35.6 wt% from the Cobalt-Gowganda ores, Canada. From the Mount Isa lead-zinc-silver ore body, "freibergite" containing 42.5 wt% silver was reported by RILEY (1974).

A mineralogical study was made on argentian tetrahedrites from Shigekuma (SHIMADA, 1971b; SHIMADA and HIROWATARI, 1972). The experimental equation of unit cell edge versus silver content presented was as follows:

$$a_0 = 10.393 + 0.0128 \cdot [\text{Ag atm\%}].$$

In addition to fourteen analyses by SHIMADA and HIROWATARI (1972), silver contents were obtained with an x-ray diffractometry for the other ten grains of tetrahedrites in the Shigekuma and Nihongi deposits (Table 11).

Accordingly, the silver content of twenty-two tetrahedrite grains in the Shigekuma deposit ranges from 3.5 to 23.8 wt%, and that of two grains from the Nihongi deposit ranges from 6.2 to 23.8 wt%.

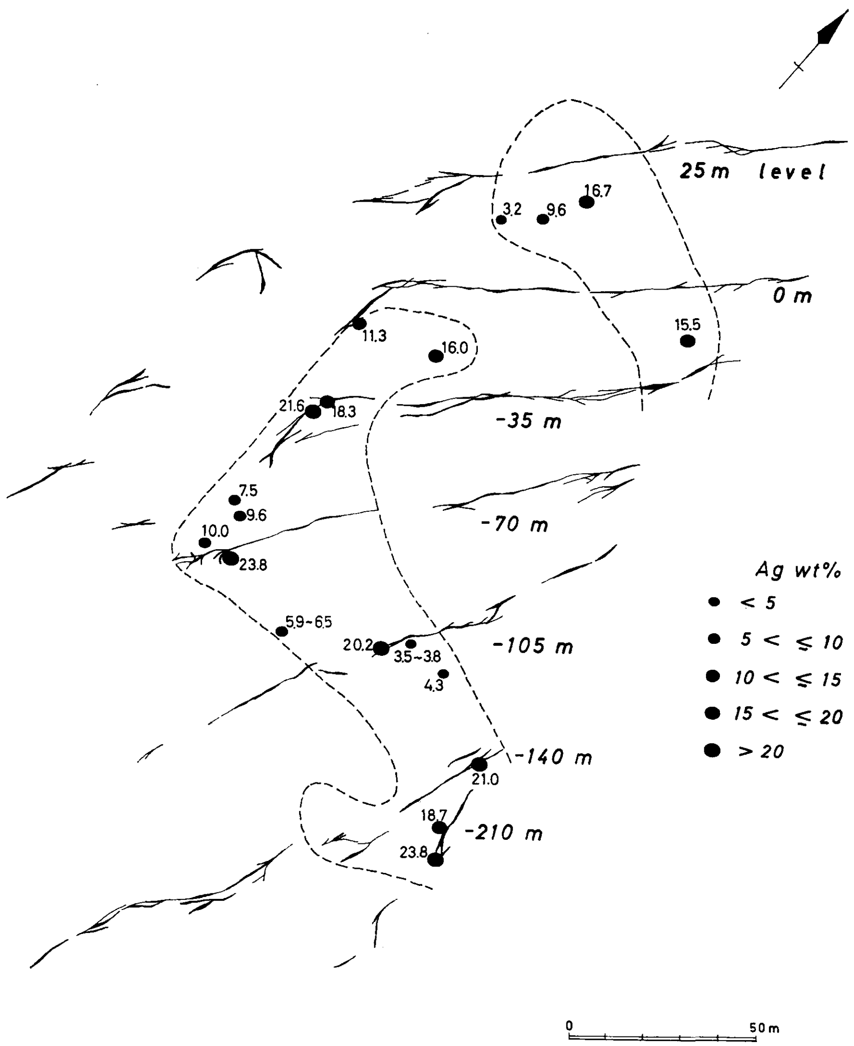


Fig. 25. Distribution of silver content (wt%) in tetrahedrites within the mineralization area of stage II (Shigekuma deposit).

*Compositional variations of tetrahedrites in Shigekuma*: From the aforementioned results, wide variations in compositions of tetrahedrites are attributed to the substitution of $Ag^+$ for $Cu^+$. Thus, the silver contents of tetrahedrites are plotted in the area of the stage II of the Shigekuma deposit (Fig. 25). In the figure, tetrahedrite relicts captured in the latter stage minerals were excluded, and the tetrahedrites plotted are regarded as products of initial deposition.

Fig. 25 indicates that the distribution of tetrahedrites has no systematic relation with their silver contents. Although the composition in a grain of tetrahedrite is rather homogeneous compared with that of the Kuroko deposits (YUI, 1971), compositional variations in different grains apart only several meters from one another are remarkable.

BERNARD (1957) studied the tetrahedrite group minerals in the Rudnany veins, Czechoslovakia, and indicated a characteristic variation with depth; contents of Hg, Ag, and Sb decrease, but those of Cu and As increase with increase of depth, and at the deepest level, Zn and Pb show maximum contents.

WU *et al.* (1974) analyzed eighty tennantite-tetrahedrite crystals from the Casapalca vein-type deposits, Central Andes of Peru, and pointed out the zoning pattern that tennantite was predominant in the central or deeper part and tetrahedrite was in the peripheral part of the ore deposits. They also indicated that silver was correlated strongly with antimony in the minerals.

It is rather common that composition of tetrahedrite series varies widely but has a systematic relation with depth. Consequently, the variational features in Shigekuma can be regarded as characteristic.

4. *Siderite*

Siderite is one of the common gangue minerals associated with lead-zinc deposits, but the occurrence of siderite, as a chief gangue from vein-type deposits in Japan, has not been much reported. NAGASAWA (1962) studied the mineralization and wall rock alteration of gold-silver-copper-lead-zinc veins of the Mikawa mine, Niigata Prefecture, and clarified that siderite had deposited in the late stage mineralization with hematite, dolomite-ankerite, kaolinite, and chlorite. The similar occurrences were also reported from such epithermal gold-silver deposits as San'ei and Nishizawa in Yamagata, Yoshiki in Gifu, Oomori in Shimane, and Hazami in Nagasaki Prefectures (Geol. Surv. Japan, 1955).

*a. The mode of occurrence of siderite in Shigekuma*

As described above, siderite is found in both the stages of I and IV. In the stage I, siderite is reddish brown, and occurs as a thin band around the breccia of mudstone (Fig. 17). In the stage IV, siderite forms compact veins having 5 to 30 cm in width. The vein includes a lot of breccias of mudstone and relicts of the former stage minerals (Fig. 26). The color of siderite is commonly yellowish brown with reddish tint.

*b. Disseminated siderite in host rocks*

Presence of siderite has been examined with x-ray powder diffraction not only on mudstone but also on fine sandstone of the host rocks around the vein. However, siderite has been scarcely found in the host rock apart more than 40 cm from the vein.

Siderite was detected substantially in mudstone at Shiohama and Ajiro, Kamishima, which had not been subjected to any kind of mineralization. Thus, siderite of sedimentary origin seems to occur widely in some specific mudstone horizons of the Taishu Group. The occurrences of mega-plant remains from Miné, Saka, Kushi, Shinsaka, Kechi, Sumo, Wakata, and Kotsuki (TATEIWA, 1934; MATSUO, 1971), and of coal seams from the west coast of Sago and the Shintomi deposit suggest that there was a sedimentary environment to yield siderite which was characterized with low Eh and neutral to weak alkaline conditions in the period of sedimentation of the Taishu Group.

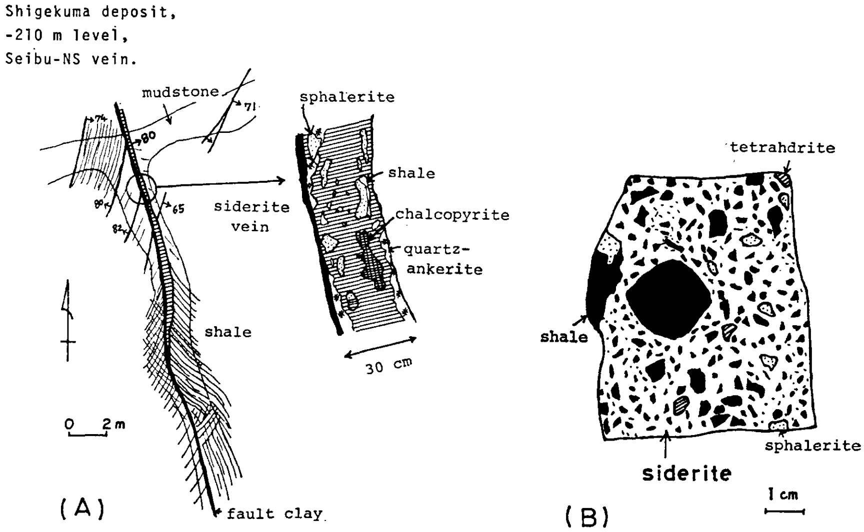


Fig. 26. Mode of occurrece of siderite vein (A), and siderite ore (B) in the stage IV.

Table 12. Chemical compositions of siderites from Shigekuma

| No. | Sample No. | FeO | MnO | MgO | CaO | $CO_2$* | Total | $FeCO_3$ | $MnCO_3$ | $MgCO_3$ | $CaCO_3$ |
|---|---|---|---|---|---|---|---|---|---|---|---|
| 1 | 604-1A | 46.8 | 4.8 | 7.7 | 1.2 | 41.0 | 101.5wt% | 69.8 | 7.3 | 20.5 | 2.4mol% |
| 2 | 604-1B | 47.2 | 3.8 | 9.3 | 0.4 | 41.7 | 102.4 | 69.2 | 5.7 | 24.4 | 0.7 |
| 3 | 604-2A | 45.4 | 6.7 | 7.7 | 1.4 | 41.5 | 102.7 | 67.0 | 10.1 | 20.3 | 2.6 |
| 4 | 604-2B | 46.4 | 4.6 | 7.7 | 1.4 | 40.7 | 100.8 | 69.8 | 7.0 | 20.6 | 2.6 |
| 5 | 609-1A | 46.1 | 3.0 | 9.0 | 0.8 | 40.6 | 99.5 | 69.6 | 4.6 | 24.3 | 1.5 |
| 6 | 609-1B | 46.8 | 4.9 | 7.7 | 1.1 | 41.0 | 101.5 | 70.0 | 7.4 | 20.4 | 2.2 |

Conditions of electron probe microanalyses: 15 kV, 0.02 micro A. Standards: $Fe_2O_3$, MnO, MgO, and $CaSiO_3$, Correction by Bence and Albee's method.
* Obtained from the calculation with stoichiometric Metal-$CO_3$.

Therefore, it is considered that siderite in sedimentary rocks was dissolved into hydrothermal solutions, and was deposited along fissures or disseminated in the neighbouring host rocks.

### c. *Chemical compositions of siderites*

Six siderites from Shigekuma were analyzed with an electron microprobe. The results are shown in Table 12. Four of them were taken from siderite veins containing large amounts of fine breccias, and the other two from veins containing some breccias. All of them analyzed are of the stage IV.

X-ray powder diffraction patterns of siderites indicate that there is no significant difference of compositions between siderites of I and IV stages.

From the above results, following conclusions are obtained: 1) Siderites in the present study are rather rich in manganese and magnesium compared with those from other localities (DEER *et al.*, 1963), as shown in Fig. 27.

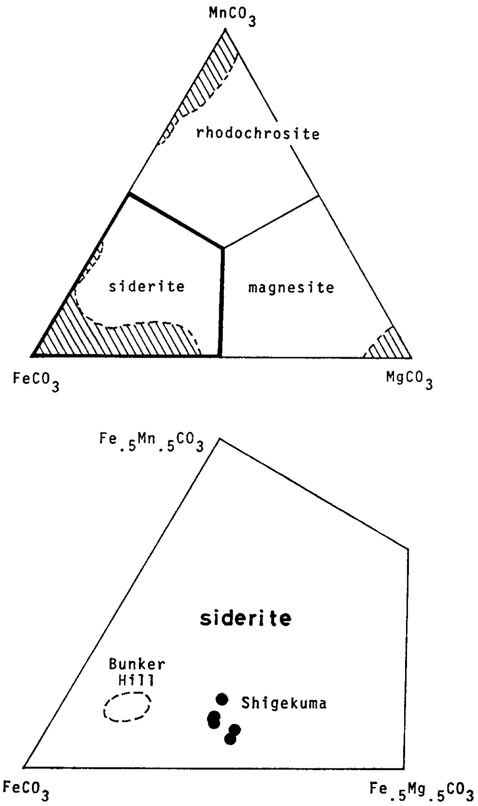


Fig. 27. Chemical composition of siderites plotted on $FeCO_3$-$MgCO_3$-$MnCO_3$ triangular diagram. Shaded area showing the region of natural calcite-type carbonates, mainly depicted from the data after DEER *et al.* (1963).

3) Chemical heterogenity both within and between grains is conspicuous. Difference of $MnCO_3$ is 3 mol% within a grain (Table 12, Nos. 3 and 4). 3) Chemical composition of siderites from Shigekuma varies widely compared with that from the Bunker Hill deposit, Coeur d'Alene district, U.S.A. (SHAW, 1959).

5. *Ankerite*

Ankerite is a variety in the series of dolomite solid solutions, and the name ankerite is here referred to a material with more than 20% of Mg site filled by Fe or Mn, after the definition of DEER *et al.* (1963).

Ankerite is fairly well known to occur with such gangue minerals as dolomite and siderite in hydrothermal deposits, especially lead-zinc veins. But mineralogical studies on ankerite in ore deposits have been scarce.

MUTA (1957b) and KINOSHITA and MUTA (1957) described the mode of occurrence and chemistry of some ankerites from the final stage of mineralization in the deposits of the Chichibu mine, Saitama Prefecture, and the Obira

Table 13. Chemical compositions of ankerites from Shigekuma

| No. | Sample No. | FeO | MnO | MgO | CaO | $CO_2$ | $Total_{wt\%}$ | $FeCO_3$ | $MnCO_3$ | $MgCO_3$ | $CaCO_{mol\%}$ |
|---|---|---|---|---|---|---|---|---|---|---|---|
| 1 | 616-1A | 13.7 | 0.2 | 12.1 | 29.0 | 44.5 | 99.5 | 18.8 | 0.3 | 29.7 | 51.2 |
| 2 | 616-1B | 17.2 | 1.0 | 9.0 | 28.5 | 43.4 | 99.1 | 24.3 | 1.5 | 22.6 | 51.6 |
| 3 | 616-2A | 13.0 | 0.2 | 13.1 | 28.2 | 44.5 | 99.0 | 17.9 | 0.2 | 32.1 | 49.8 |
| 4 | 616-2B | 16.5 | 0.3 | 10.5 | 27.9 | 43.7 | 98.9 | 23.2 | 0.5 | 26.2 | 50.1 |
| 5 | 616-3A | 9.1 | 0.2 | 15.4 | 29.4 | 45.5 | 99.6 | 12.2 | 0.2 | 36.9 | 50.7 |
| 6 | 616-3B | 13.1 | 0.1 | 12.6 | 28.7 | 44.5 | 99.0 | 18.1 | 0.2 | 31.0 | 50.7 |
| 7 | 616-3C | 17.5 | 0.9 | 8.8 | 28.3 | 43.0 | 98.5 | 24.9 | 1.2 | 22.2 | 51.7 |
| 8 | 624-1A | 16.5 | 2.6 | 8.1 | 28.9 | 43.2 | 99.3 | 23.3 | 3.8 | 20.4 | 52.5 |
| 9 | 624-1B | 15.5 | 1.2 | 10.4 | 28.3 | 43.9 | 99.3 | 21.7 | 1.7 | 25.9 | 50.7 |
| 10 | 624-1C | 14.2 | 0.6 | 11.4 | 27.8 | 43.3 | 97.3 | 20.1 | 0.8 | 28.8 | 50.3 |
| 11 | 624-2A | 15.3 | 1.3 | 10.1 | 29.7 | 44.5 | 100.9 | 21.0 | 1.8 | 24.8 | 52.4 |
| 12 | 624-2B | 16.0 | 1.1 | 9.8 | 29.8 | 44.5 | 101.2 | 21.9 | 1.5 | 24.1 | 52.5 |
| 13 | 243-3A | 13.4 | 0.2 | 12.9 | 29.8 | 45.8 | 102.1 | 17.9 | 0.2 | 30.8 | 51.1 |
| 14 | 243-3B | 13.3 | 0.1 | 13.7 | 29.6 | 46.4 | 103.1 | 17.5 | 0.1 | 32.3 | 50.1 |
| 15 | W719-A | 17.8 | 0.6 | 7.9 | 30.0 | 43.4 | 99.7 | 25.2 | 0.8 | 19.9 | 54.1 |
| 16 | W719-B | 18.2 | 0.7 | 7.9 | 30.4 | 44.1 | 101.3 | 25.3 | 0.9 | 19.7 | 54.1 |
| 17 | W717-A | 15.0 | 0.7 | 9.4 | 31.2 | 44.4 | 100.7 | 20.8 | 1.0 | 23.0 | 55.2 |
| 18 | W717-B | 7.9 | 0.1 | 16.8 | 32.9 | 49.1 | 106.8 | 9.9 | 0.2 | 37.3 | 52.6 |
| 19 | W719H2 | 16.1 | 0.3 | 8.7 | 30.5 | 43.5 | 99.1 | 22.7 | 0.5 | 21.8 | 55.0 |

Localities: Nos. 1 to 7: −70m level, Chubu N-S vein. Nos. 8 to 12: −140m level, Honpi vein, Nos. 13 and 14; 0m level, spot 28, Nos. 15 to 19: cross-cutting gallery, 0m level, Shigekuma deposit.
Analytical conditions were the same as those in Table 12.

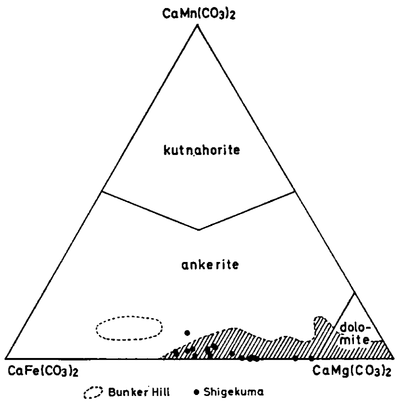


Fig. 28. Chemical composition of ankerites from Shigekuma, plotted on $CaMn(CO_3)_2$-$CaFe(CO_3)_2$-$CaMg(CO_3)_2$ diagram. Shaded area shows the frequency over 1.65% of natural dolomite-type carbonates (MINCHEVA-STEFANOVA, 1970).

mine, Oita Prefecture. SHAW (1959) reported the paragenesis and chemical compositions of ankerites from the Bunker Hill mine, Idaho.

*a. Chemical compositions of ankerites*

Nineteen ankerite grains from Shigekuma were analyzed with an electron microprobe. The results are shown in Table 13, and are also plotted on the

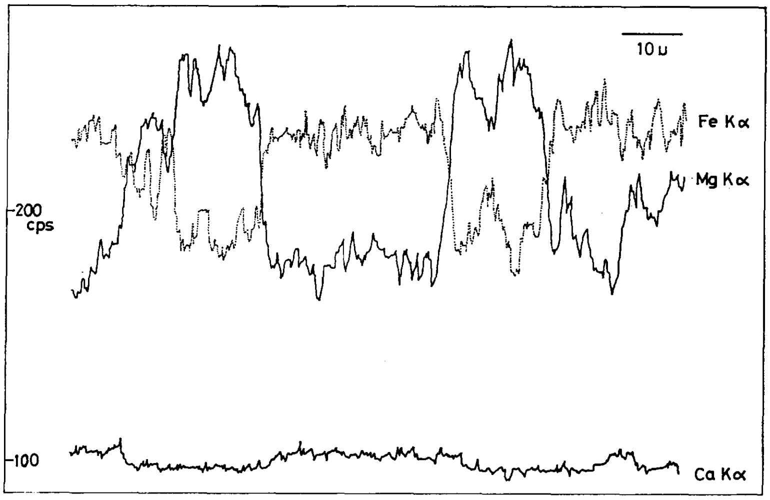


Fig. 29. Line scans with an electron microprobe on ankerite veinlet from Shigekuma. The difference between maximum and minimum intensities corresponds to about 20 mol% $CaFe(CO_3)_2$.

triangular diagram (Fig. 28). The chemical formula of the present ankerites can be expressed as follows:

$$Ca_{1.00-1.10}(Fe_{0.20-0.51}Mg_{0.39-0.75}Mn_{0-0.07})(CO_3)_2$$

Fig. 28 indicates that ankerites in Shigekuma have very wide range of composition, and occupy a large area in the frequency distribution of natural dolomite-type carbonates, reported by MINCHEVA-STEFANOVA (1970). The present ankerites have an extremely wider range of composition than that of ankerites from the Bunker Hill mine.

The variation of chemical composition of ankerites is recognized not only in a single veinlet but also in a single grain. The variation in a veinlet shown by the analyses of Nos. 1 to 7, and so on, and that in a grain is shown by a profile of line scans taken with an electron microprobe (Fig. 29). Therefore, it is concluded that the composition of ankerite is fairly inhomogeneous.

*b. X-ray investigation of ankerites*

X-ray powder diffraction patterns of ankerites from Shigekuma, Nihongi, Kanayama, and other deposits in Kamishima agree well with that reported by HOWIE and BROADHURST (1958). They show weak ordered *hkl* reflections, which are observed when $h+k+l+2n+1$ and $h=k$ or $k=l$ or $l=h$. As the spacing of $d(211)$ of dolomite-ankerite series is largely influenced by the amount of substitution of iron or manganese for magnesium, the $d(211)$ spacings of seventy-nine ankerites were measured using the 101 reflection of associated quartz as an internal standard. They range from $2.89_3$ to $2.91_4$ Å. The larger value of the spacing means the higher iron or manganese content in ankerite.

*c. Variations of the chemical compositions of ankerites around the ore veins*

At the two cross-cutting galleries, 0 m and −140 m levels in the Shigekuma

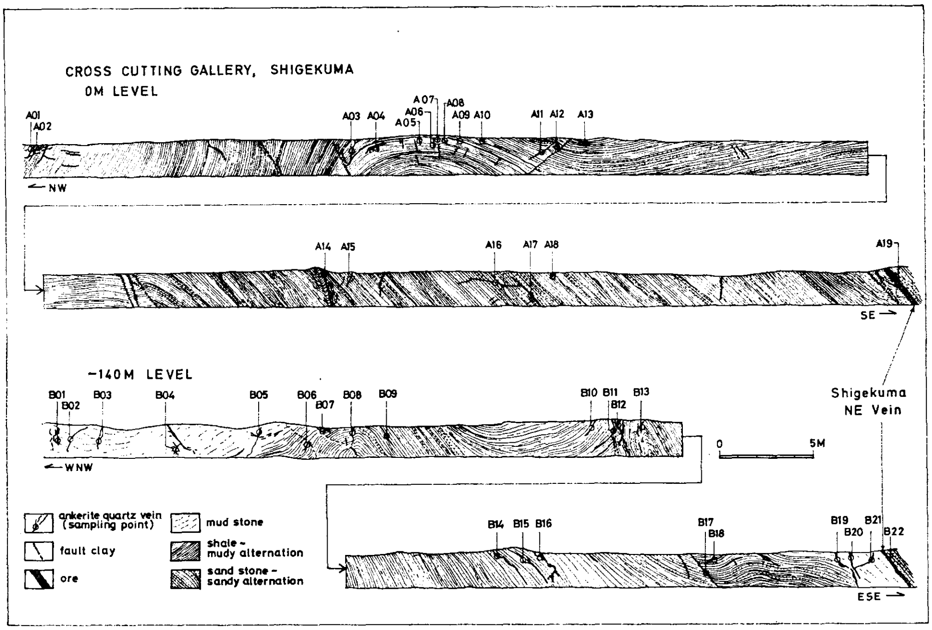


Fig. 30. The mode of occurrence and sample localities of ankerites in the cross-cutting galleries at 0 m and −140 m levels, Shigekuma deposit.

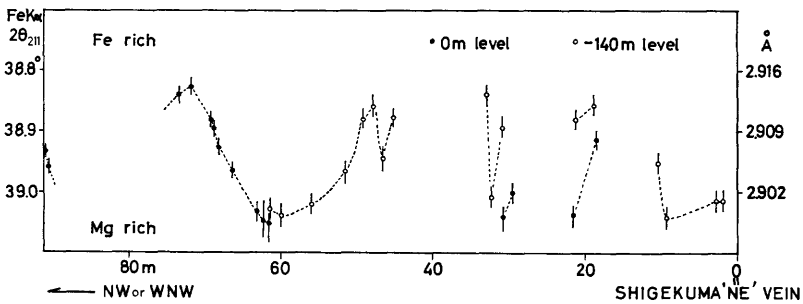


Fig. 31. Variation of $d(211)$ spacings of ankerites taken from the galleries as shown in Fig. 30.

deposit, numerous veinlets of quartz-ankerite occur around the ore veins as shown in Fig. 30. The composition of ankerite was estimated from the value of $d(211)$, and was plotted on Fig. 31. The figure indicates that the composition varies widely within several meters, and sometimes continuously. However, the compositional variation in ankerites of both the levels is in nearly the same range. Thus, it is concluded that the composition of ankerites is not affected or controlled by the distance from the ore vein or with depth.

*d. Variation in the compositions of ankerites in the cores of borehole*

Numerous carbonate veinlets were also observed in the cores of the borehole, taken at Chihira, Sago area (Fig. 5). The veinlets attain to 3 cm in width.

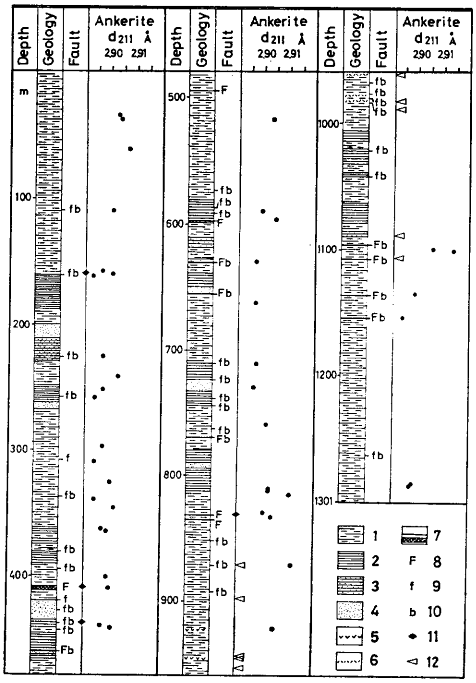


Fig. 32. Variation of $d(211)$ spacings of ankerites taken from the bolrehole at Chihira. 1: mudstone, 2: shaler-ich alternation, 3: sandstone-rich alternation, 4: sandstone, 5: dolerite, 6: tuff, 7: fault, 8: major fault with fault clay more than 30 cm in width, 9: minor fault, 10: bedding-plane fault, 11: sphalerite and galena ore, 12: calcite veinlet.

They are composed of carbonate minerals and quartz, and partially contain the relict of sphalerite and galena in the depth of 410 to 441 m, within the sheared zone of Gozaemon Fault (MITI, 1975).

X-ray powder diffractometry showed that the fourty-four samples were composed of ankerites, and the ten samples from the depth 872 to 1,106 m were calcites. It is interesting that the occurrence of calcite vein has never been found in Kamishima except this place. This fact will be discussed in later with the relation to carbonate zoning.

The spacing values of $d(211)$ were measured on a large number of ankerites and were plotted on Fig. 32. The histogram of the data is also depicted in Fig. 33. Judging from the results, the composition of ankerite shows no regular change with depth or with distance from major fault, which is accompanied by some lead-zinc mineralization. The variation of the composition of ankerites may occur at random within a narrow place less than a few meters.

*e. Formation environment of ankerites*

A summary of the results obtained for ankerites is as follows: 1) Ankerite occurs in association with quartz along fissures around the ore veins of Kamishima. It generally deposited after lead-zinc mineralization. 2) Ankerite takes

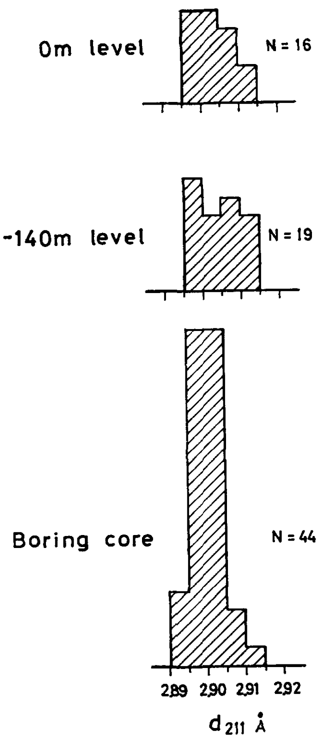


Fig. 33. Histogram of $d(211)$ spacings of ankerites.

an extremely wide range in composition, and has the following formula:

$$Ca_{1.00-1.10}(Fe_{0.20-0.51}Mg_{0.39-0.75}Mn_{0-0.07})(CO_3)_2$$

3) Chemical composition of ankerite varies widely even in a single grain, and the bulk composition of ankerite veinlets varies continuously and widely within several meters.

From these results, it can be concluded that the composition of ankerite does not vary systematically with depth or with distance from ore veins, which are main path of the ore-forming solutions. Accordingly, the ore-forming solutions are inferred to have formed ankerite as a metastable phase by rapid escape of $CO_2$ from numerous open fissures. Therefore, ankerite seems to be a product under far from equilibrium condition.

This conclusion is also elucidated by some discrepancies between natural and synthetic ankerites. ROSENBERG (1967) has indicated by his synthetic data that the content of iron in dolomite solid solutions increases with increasing temperature from 350° to 550°C, in 2 to 3 kilobars. This trend bears some resemblance with the experimental data by GOLDSMITH *et al.* (1962). But wide variation in the composition of the present ankerites in a small scale would not correspond to the temperature difference of some hundreds degrees. SHCHERBAN' and SHIROKIKH (1971) have indicated that association of natural ankerite and amorphous silica is stable only below the temperature of 225°C, which is

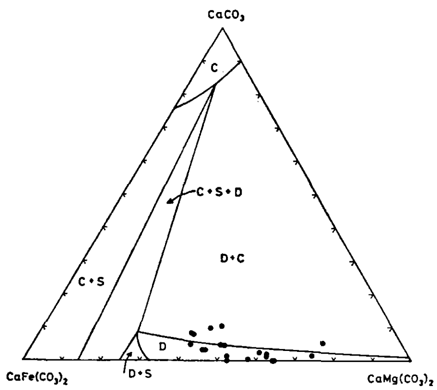


Fig. 34. Composition of ankerites analyzed, plotting on the diagram of the system $CaCO_3$-$MgCO_3$-$FeCO_3$ at 450°C presented by ROSENBERG (1967). C: calcite solid solution, D: dolomite solid solution, S: siderste-magnesite solid solution, Filled circle: ankerites from Shigekuma.

consistent with the fluid inclusions data, as described later.

When plotting the compositions of ankerites in the phase relations presented by ROSENBERG (Fig. 34), they mostly occupy the region of dolomite solid solutions, but five are in the dolomite + calcite region. However, none of ankerites plotted are associated with calcite. This is another discrepancy between natural and synthetic ankerites.

## E. Zoning of carbonate minerals

In the Shigekuma deposit, siderite occurs as massive veins, and also as disseminated rocks around the ore veins. The association of ankerite and quartz is dominant in fissures away from ore veins, as shown in the cross-cutting galleries, and also in the cores of borehole (Fig. 30 and 32). Calcite is found only as veinlets at the deepest part of the borehole (Fig. 32). As Gozaemon Fault shows dip of 80°E, calcite veinlets occur in the region outer than 150 m from the fault, which contains mainly the ore minerals in the borehole.

Thus the carbonate zoning is observed among minerals of the stage IV in Shigekuma-type mineralization: siderite in the central, ankerite in the middle, and calcite in the marginal zones. The pairs of siderite-ankerite and ankerite-calcite are slightly found along the boundary of each zone. This zonal distribution seems to be resulted from hydrothermal differentiation during mineralization.

## F. Fluid inclusions

Fluid inclusion study was made on quartz in the stage IV of the Shigekuma deposit. The samples were cut and polished into plates of 0.1 to 0.3 mm thick. Inclusions take oval or elongated irregular shape, with size under 30 microns. They have two phases, vapor and liquid. Inclusions composed of three phases have not been observed, although inclusions having $CO_2$ liquid, aqueous solution, and vapor were reported from Shigekuma (IMAI *et al.*, 1971; IMAI and TAKENOUCHI, 1973).

Homogenization temperatures were measured in air on a Union MHS-3 type heating stage, using a chromel-alumel thermocouple. When the inclusions were heated, the vapor bubble disappeared. The results of six inclusions indicate that the homogenization temperatures range from 208° to 222°C.

### G. Peculiarities of Shigekuma-type mineralization

Characteristics of the mineralization of the Shigekuma-type are summarized as follows:

1) Ore deposits in Kamishima are essentially narrow silver-lead-zinc veins, and are distributed in three areas, Sago, Nita-Miné, and Kin areas.

2) They are developed in fissures along N-S sheared faults (lefthanded strike-slip ones), NE faults (bedding-plane reverse ones), and NW tension faults.

3) Localization of ores is controlled by the distribution of competent rocks, because fissures are dominant around the faults intersecting across such rocks as sandstone, plagiophyre and dolerite.

4) No igneous rocks related to the mineralizations crop out in the vicinities of the three areas, except a cryptobatholith which may be distributed at 7 km northwestwards away from the Kanayama deposit, Kin area.

5) Ore deposits in Kamishima are generally characterized by mineral assemblage of Fe-poor sphalerite, finely foliated galena, pyrite, Fe-carbonate minerals and quartz, though the Shigekuma deposit yields also subordinate amounts of argentian tetrahedrite and chalcopyrite.

6) The veins, in general, include a lot of fine grained breccias composed of host rocks.

7) Mineral sequence has been established, and divided into four stages, namely, Zn-Fe stage (I), Cu-Ag stage (II), Pb stage (III), and Fe-carbonate stage (IV).

8) Almost all of the deposits commonly lack the stage II, or Cu-Ag mineralization, except Shigekuma and Nihongi deposits.

9) Throughout the mineral sequence from stage I to III in Shigekuma, localization of minerals of younger stage is confined to the area of older one. Mineralization of the stage IV superposes the former products, and moreover extends outwards to form carbonate zoning, namely, central siderite zone, middle ankerite zone, and marginal calcite zone.

10) The mineralization related to tectonic causes can be regarded as the tectonic opening-type zonality in SMIRNOV's sense.

11) Chemical compositions of major constituent minerals show no systematic variation vertically and laterally in each mineralization stage.

12) Homogenization temperatures of fluid inclusions in quartz are indicated to be 208° to 222°C.

## IV. Taishu-type mineralization

Although metalliferous ore deposits are found in five areas in Shimojima,

Table 14. Optical and physical properties of tetradymite ($Bi_2Te_2S$) and tellurobismuthite ($Bi_2Te_3$) from Yoranaiin

| | tetradymite | tellurobismuthite |
|---|---|---|
| Color | white, with a light green tint | white, with a creamy tint |
| Reflectivity | very high <tellurobismuthite | very high >tetradymite |
| Bireflectance | weak | very weak |
| Anisotropy | distinct | distinct |
| Internal reflections | not present | not present |
| Cleavage | perfect//(0001) | perfeft//(0001) |
| Polishing hardness | <tellurobismuthite | >tetradymite |
| $VHN_{10}$ | 46-61 | 60-67 |

Table 15. Chemical compositions of tetradymite and tellurobismuthite from Yoranaiin

| Sample | Bi | Sb | Te | S | Total | Chemical formula |
|---|---|---|---|---|---|---|
| 1 | 60.9 | 0.2 | 34.2 | 4.1 | 99.4 | $(Bi_{2.11}Sb_{0.01})_{2.12}Te_{1.95}S_{0.93}$ |
| 2 | 60.7 | 0.2 | 35.2 | 4.2 | 100.3 | $(Bi_{2.08}Sb_{0.01})_{2.09}Te_{1.97}S_{0.94}$ |
| 3 | 60.3 | 0.3 | 34.8 | 3.9 | 99.3 | $(Bi_{2.10}Sb_{0.02})_{2.12}Te_{1.99}S_{0.89}$ |
| 4 | 52.9 | 0.4 | 45.4 | 0.0 | 98.7 | $(Bi_{2.06}Sb_{0.03})_{2.09}Te_{2.91}$ |
| 5 | 52.4 | 0.4 | 45.7 | 0.0 | 98.5 | $(Bi_{2.05}Sb_{0.03})_{2.08}Te_{2.92}$ |
| 6 | 52.9 | 0.4 | 45.8 | 0.0 | 99.1 | $(Bi_{2.05}Sb_{0.03})_{2.08}Te_{2.92}$ |

Nos. 1 to 3: tetradymite, Nos. 4 to 6: tellurobismuthite

the denser distribution is found in Sasu area or Taishu mine where high grade ores are impregnated in large scale. The mineralization of each area in Shimojima will be briefly described as follows:

## A. Mineralization in Yora area

The greisen-like veins are found in some boulders at Yoranaiin, Yora area. They are chiefly composed of tourmaline, euhedral apatite, $2M_1$-muscovite, chlorite, quartz, amethist, and a small amount of cobaltite, tetradymite, and tellurobismuthite.

The optical properties and chemical compositions of tetradymite and tellurobismuthite are shown in Tables 14 and 15.

Chemical compositions of cobaltite were obtained with an electron microprobe, and are shown in Table 16. According to the experiment of FeAsS-NiAsS-CoAsS system by KLEMM (1965), the formation temperature of cobaltite is estimated to be 370° to 400°C (Fig. 35).

Apatite crystals contain fluid inclusions with vapor and liquid phases. Homogenization temperatures of five samples show 255° to 280°C.

From the modes of occurrence of the minerals and observations under a microscope, the mineral sequence of the area has been determined as shown in Fig. 36.

The mineralization is characterized by high temperature minerals and rather specific mineral assemblage, but is considered to correspond to the Co-As stage

Table 16. Chemical compostions of cobaltite from Yoranaiin

| Sample | Co | Fe | Ni | As | S | Total | Chemical formula |
|---|---|---|---|---|---|---|---|
| A | 31.1 | 4.1 | 2.2 | 42.6 | 19.3 | 99.3 | $(Co_{0.88}Fe_{0.12}Ni_{0.06})_{1.06}As_{0.94}S_{1.00}$ |
| B | 30.0 | 4.5 | 3.0 | 43.1 | 19.1 | 99.7 | $(Co_{0.84}Fe_{0.13}Ni_{0.09})_{1.06}As_{0.95}S_{0.99}$ |

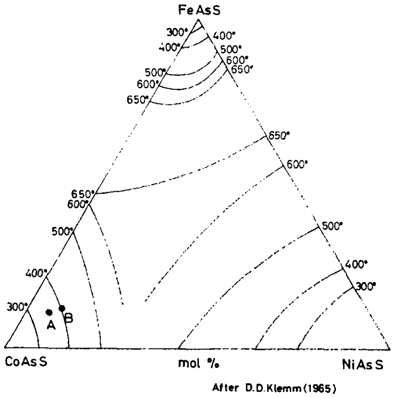


Fig. 35. The formation temperature of cobaltite from Yoranaiin, obtained by the diagram of KLEMM (1965).

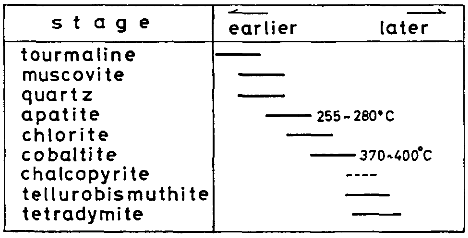


Fig. 36. Mineral sequence of Yora area.

in Sasu area. As the area is located in hornfels zone closer than some hundreds meters from biotite granite, the mineralization is intimately related to the granite intrusion.

## B. Mineralization in Sasu area

### 1. *Hypogene mineralization*

Dominant mineralization of the area is divided into following three stages on the basis of such structures as crustification and intersecting: the stage I or Co-As stage, the stage II or Fe-Zn-Pb stage, and rejuvenation stage.

*Co-As stage*

The first stage is characterized by the presence of high temperature minerals and also by the dominant precipitation of calcite. The following succession of the mineral sequence has been observed.

1) Deposition of abundant quartz accompanied by tourmaline (Kune-Toobu deposit).

2) Deposition of quartz accompanied by cobaltite and arsenopyrite (Furukawa deposit).

3) Deposition of quartz and arsenopyrite accompanied by small amounts of chalcopyrite and chlorite (Motoyamamichi, Yasuda-Taisho, and Misumiyama-Higashi deposits).

4) Deposition of barren quartz (bottom part of the Shintomi, Himi, and Yasuda-Taisho deposits).

5) Deposition of large amounts of calcite (especially Tsurue, Himi Nos. 1 and 2 Uwaban deposits).

The succession from Nos. 1 to 5 indicates the paragenetic variation with distance from biotite granite, although the deposition relation between quartz and calcite is indefinite.

Calcite is abundantly found in the Tsurue deposit, and also in the Himi Nos. 1 and 2 Uwaban deposits, which were formed along tension fractures trending NNW to NW. Solubility of calcite decreases markedly with decreasing the partial pressure of $CO_2$ (HOLLAND and BORCSIK, 1965). Therefore, it seems that such tension fractures and faults could be suitable for calcite deposition.

*Fe-Zn-Pb stage*

The second stage contains large amounts of pyrrhotite, sphalerite, and galena, associated with small amounts of chalcopyrite, pyrite, arsenopyrite, native bismuth, some sulfosalt minerals, quartz, calcite, chlorite and sericite.

Abundant breccias of calcite and minor amounts of quartz of the former stage are observed as captured fragments in pyrrhotite-sphalerite-galena ores of the Urakochi-Somen deposit, and also in ores of −140 m levels of the Kunoe deposit, −210 m to −280 m levels of the Himi deposit, and the Shimoken deposit. Calcite veins of the former stage are clearly cut by massive sphalerite-galena veins in the Himi Nos. 1 and 2 Uwaban deposits and the Taihei old adit.

Assay maps of major deposits in the area show that the mineral contents of pyrrhotite, sphalerite, and galena in ores change gradually with depth (UEHARA, 1959a, 1964; MATSUHASHI, 1968). According to the association of major minerals, the zoning pattern is depicted as pyrrhotite zone, pyrrhotite-sphalerite zone, sphalerite-galena zone (sphalerite>galena), and sphalerite-galena zone (galena>sphalerite) in ascending order as shown in Fig. 37.

At the boundary of each zone, there is usually gradual change of mineral composition. This type of zoning is fairly correlated to "deposition-type zonality" of SMIRNOV (1960). The zonality is considered to be greatly related to physico-chemical parameters, which regulate the deposition of minerals from ore-forming solutions. A drop of temperature is inferred to be the most effective parameter.

Pyrrhotites including hexagonal and monoclinic types and their mixtures are reported from ores of the Kunoe, Akushidani, and Yasuda-Taisho deposits (MUKAIYAMA and IZAWA, 1966). X-ray diffractometry indicates that the structure type of pyrrhotite is monoclinic type only in the Shiratake-Uwaban deposit, which is located at the northern part of the area. It is roughly stated that monoclinic pyrrhotite abounds in the deposits far from biotite granite. According to MUKAIYAMA (1965), however, the variation of iron content and structure of pyrrhotite has no regularity with depth in the Kunoe deposit.

Every sphalerite in ores of the area is iron-rich variety or marmatite. The content of FeS in sphalerites ranges from 9 to 27 mol% in Himi, Shintomi, Misoge, and some other deposits (MUTA, 1958a; MUKAIYAMA and MIKURIYA, 1964). The chemical variation of sphalerite is conformable with the zoning pattern, namely the iron content generally decreases with decreasing depth in an ore body.

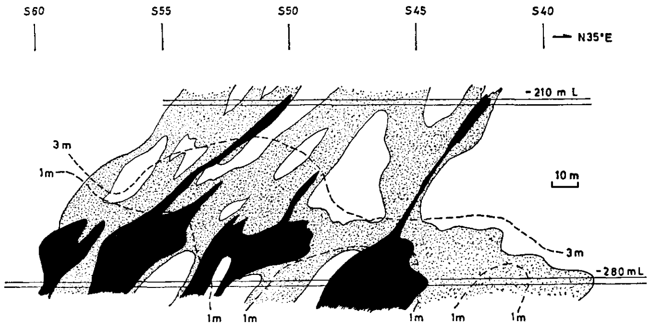


Fig. 38. The rejuvenation stage (filled area) intersecting across the Fe-Zn-Pb stage (dotted area) at the southern part of the Senninmabu-Sosen deposit. Dotted line: thickness of the sandstone beneath the ores (The perspective profile modified after KURONUMA, C.).

According to detailed investigation on fluid inclusions (IMAI *et al.*, 1971), homogenization temperatures of inclusions in quartz from the area indicate 150° to 370°C, and their salinity ranges from 5 to 33 wt% NaCl equivalent. Almost all the quartz crystals are considered to belong to the Fe-Zn-Pb stage judging from their localities.

2. *Rejuvenation stage*

In the Senninmabu-Somen deposit, the largest one in the area, the rejuvenation stage is observed at the two deepest parts. The presence of the stage is fully expressed in Fig. 37, because the pattern of the deposition-type zonality is disturbed at these parts.

The vein of this stage clearly intersects across the former products and also superposes on them. The vein is composed of very fine grained compact ores being less than 50 cm in width, from which the coarse grained mineral assemblage of the former Fe-Zn-Pb stage is easily distinguished. The minerals are fine mixture of pyrrhotite, sphalerite and galena. No grains or inclusions of chalcopyrite are found in the ores of the rejuvenation.

At the spots of S60 to S40 on the levels of −210 m to −280 m of the Senninmabu-Somen deposit, the area of the rejuvenation stage is shown together with that of the Fe-Zn-Pb stage in Fig. 38. As the deposit is formed along a bedding-plane reverse fault, the thickness of the sandstone underlying the ores is also indicated in Fig. 38. It is ascertained that the rejuvenation occupies the place where the thickness becomes thinner and cross lamination is well developed. Accordingly, the reopening of fissures is inferred to have been controlld by the sedimentary structure of sandstone, even after the fracture had been filled with ore veins of the Fe-Zn-Pb stage.

So far to date, the presence of rejuvenation has never been known except these two parts, but it may probably be found at the deeper horizons of other deposits.

3. *Secondary alteration*

Not only pyrrhotite-rich ores of the Akushidani deposit but also sphalerite-

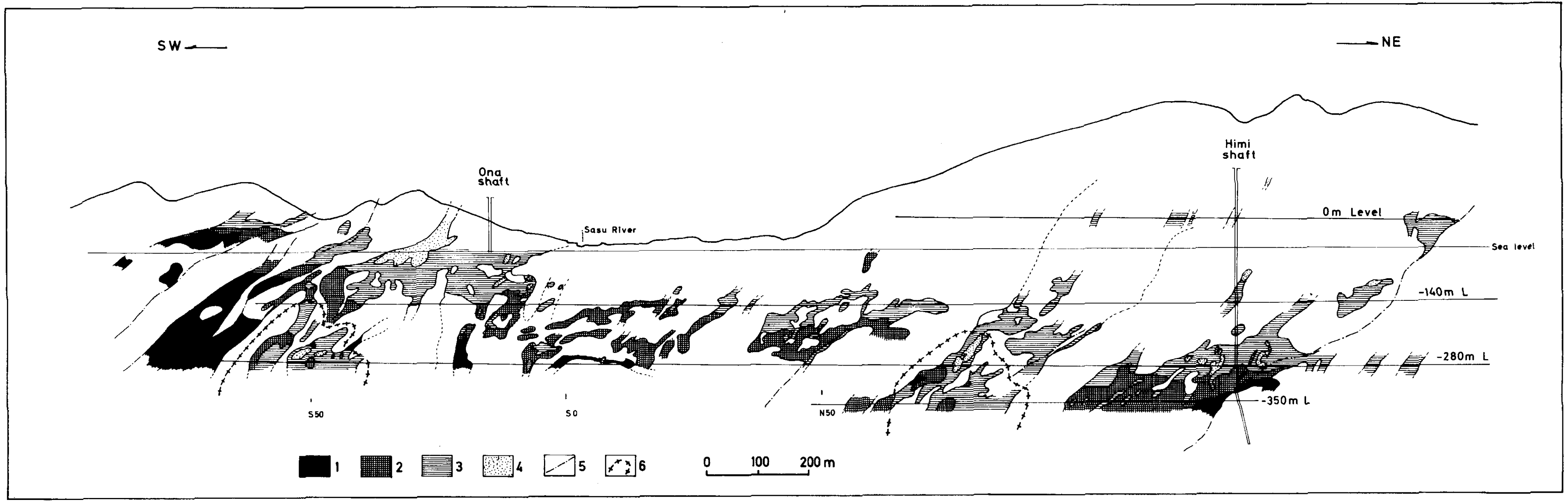


**Fig. 37.** Deposition-type zonality on the perspective section of the Senninmabu-Somen deposit, Sasu area (modified after the Toho Zinc Company).

1: pyrrhotite zone, 2: pyrrhotite-sphalerite zone, 3: sphalerite-galena zone (sphalerite>galena), 4: sphalerite-galena zone (galena >sphalerite), 5: intersecting line between N-S fault and NE one, 6: the area of rejuvenation superposing on the former stage.

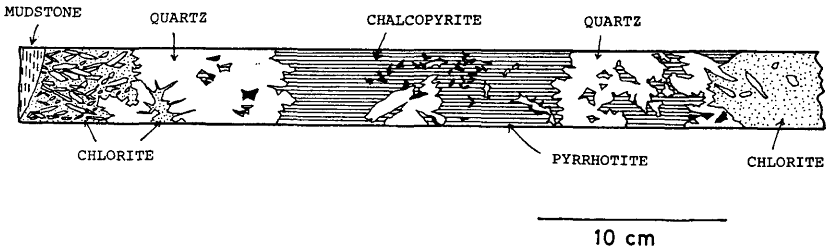


Fig. 39. The inter-vein structure of the deposit in Ohfunakoshi area.

galena ores of the Aré-Somen, Himi, Misoge, and other deposits have been weakly but widely affected by the secondary alteration. The products are found as veinlets filling hair cracks of the hypogene ores. They are mainly composed of colloform pyrite, fine grained aggregate of marcasite and carbonates, quartz, siderite, and calcite.

## C. Mineralization in Ohfunakoshi area

On the specimens obtained at many outcrops and some old adits, and also on the cores of two boreholes (MITI, 1975), the modes of occurrence of the vein-forming minerals and their properties have been studied.

The inter-vein structure is characterized by abundant comb structure of quartz as shown in Fig. 39.

The veins are mainly composed of quartz and pyrrhotite, accompanied by arsenopyrite, chalcopyrite, sphalerite, galena, calcite, chlorite and sericite. Chlorite occurs abundantly as gangue minerals compared with other veins in Tsushima.

The series of mineralization is considered to be started with quartz and chlorite, followed by arsenopyrite, pyrrhotite, native bismuth, chalcopyrite, sphalerite, and galena. Pyrite and calcite are generally later than those minerals. Exsolved skeletal sphalerite is commonly found in chalcopyrite and pyrrhotite.

Homogenization temperatures were measured with a heating stage on eighteen fluid inclusions in quartz from the Konjobana deposit. The result shows that they range from 295° to 378°C.

Because the veins are impregnated in the places close to hornfels as described before, the mineralization is considered to be intimately related to a cryptomass of granite. The features of ore deposits are quite similar to those of the Sasu area, especially to Akushidani and Shimoken deposits in mineral assemblage, texture of ore minerals, homogenization temperature, and close affinity to granite. However, the features differ somewhat on the following points: The Ohfunakoshi deposit contains pyrrhotite and arsenopyrite ores which show a high silver content up to 300 g/ton, though lead content is very low. The deposits generally abounds in pyrrhotite ores, but accompany narrow branch veins of sphalerite, galena and/or calcite.

Thus it is concluded that the mineralization of the area is featured by telescoping of such mineralization in Sasu area.

### D. Mineralization in Izuhara and Tsutsu areas

Ore deposits and outcrops of these areas are composed of marked tourmaline veins, pyrrhotite ores, and sphalerite and galena veins. The Nariaisai deposit abounds in sphalerite and galena but accompanies a molybdenum-bearing mineral like wulfenite. Thus the mineralization of the area may roughly be regarded as telescoped mineralization derived from nearly the same source as Sasu area.

### E. Mineralization in Shimojima

Mineralizations in Shimojima, which are here called Taishu-type mineralization, are summarized as follows:

1) Ore deposits in Shimojima are composed mainly of lead-zinc iron sulfide veins, which are distributed in five areas, namely, Sasu, Tsutsu, Yora, Izuhara, and Ohfunakoshi areas.

2) They are impregnated in fissures along faults, trending N-S, NE and NW, whose patterns are mostly the same as those in the ore deposits in Kamishima or the Shigekuma-type.

3) In Sasu area, lead-zinc ore deposits are densely developed. Hypogene mineralization of the area is composed of three stages: Co-As, Fe-Zn-Pb, and rejuvenation stages.

4) Mineralization of the Co-As stage features lateral or district zoning, and that of the Fe-Zn-Pb stage shows marked deposition-type zonality.

5) Various deposits in Ohfunakoshi, Izuhara, and Tsutsu areas are regarded as those consisting of telescoped ores of the mineralizations in Sasu area. Mineralization in Yora area is characterized by greisen-like veins, which correspond to the Co-As stage in Sasu area.

6) All the metalliferous ore deposits in Shimojima are genetically related to biotite granite, which crops out at Uchiyama and Hikage and also creeps into the crest of anticline at Izuhara and Ohfunakoshi areas.

## V. Considerations

### A. Lead-zinc mineralization in Tsushima

Above results have clarified that there occur two distinct types of lead-zinc ore deposits in Tsushima: Shigekuma-type and Taishu-type ore deposits. Comparison of these two types is summarized in Table 17.

Both the types of mineralization were yielded by three or four interrupted ascent of ore-forming solutions, caused by serial or interrupted fracturing and reopening of fissures. One stage of the Shigekuma-type mineralization exhibits no depositional zonality like Taishu-type.

Shigekuma-type mineralization is characterized by the tectonic opening-type zonality as shown schematically in Fig. 40, low temperature mineral association, and also variable chemical composition of main constituent minerals. It is inferred that the mineralization of Shigekuma-type was highly affected by an accidental event, such as boiling and throttling of the ore-forming solution along

Table 17. Comparison of mineralizations between Shigekuma-type and Taishu-type

| | Taishu-type | Shigekuma-type |
|---|---|---|
| Hypogene ore mineral | sphalerite, galena, pyrrhotite, chalcopyrite, arsenopyrite, (cobaltite, Bi-Te minerals) | sphalerity, galena, tetrahedrite, pyrite, chalcopyrite, (bounonite, ullmannite) |
| Gangue mineral | quartz, calcite, (tourmaline, chlorite, sericite) | quartz, siderite, ankerite, (calcite, chlorite, sericite) |
| Silver content per 1% Pb | 20 gram/ton | 100 gram/ton |
| FeS content in sphalerite | 27-9 mol% | 5-1 mol% (Kanayama; 13-8) |
| Variation of FeS content in sphalerite with depth | systematic | random |
| Characteristic zonality | facies zonality (deposition-type) | stage by stage zonality (tectonic opening type) |
| Homogenization temperature | 378°-150°C | 222°-208°C |
| Igneous rock related to mineralization | biotite granite | unknown |

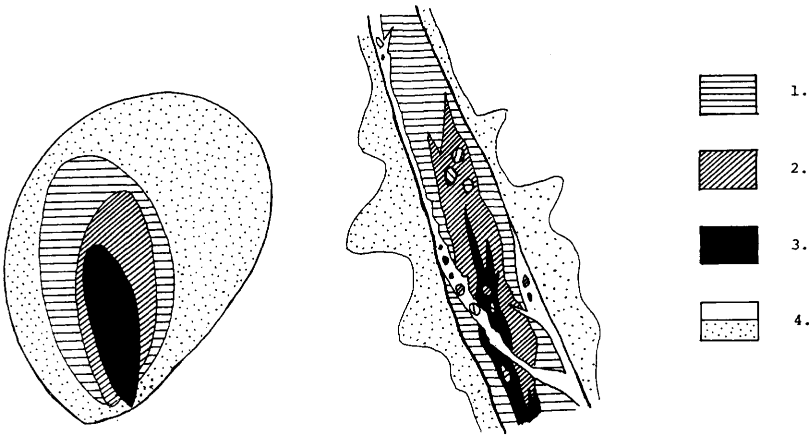


Fig. 40. Idealized diagram showing the tectonic opening zonality in the Shigekuma deposit. 1: stage I, 2: stage II, 3: stage III, 4: compact vein composed mainly of siderite (open area), and dispersed mineralization area composed mainly of ankerite (dotted area) of the stage IV.

the conduit, judging from the inter-vein structure and the variable chemical composition of minerals.

Formation of the remarkable deposition-type zonality of the Taishu-type deposits is well explained by mixing of ore-forming solution with connate and meteoric water, as suggested by the fluid inclusion study of IMAI *et al.* (1971).

IMAI and TAKENOUCHI (1973) considered that ore-forming solution had originated from granite. But, it may also be possible that almost all the metals composing the deposits have been derived from thermally metamorphosed mudstone of the Taishu Group. By the intrusion of biotite granite, dehydration should had taken place within hornfels zone. Solutions supplied by the dehydration might contain substantial amounts of metal and chlorine, leached out from the hornfels zone of mudstone, although further study is needed.

## B. Metallogenic situation of Tsushima in the belt of Ryukyu arc

Concerning the Neogene metallogenic provinces in Japan, lead-zinc ore deposits of Tsushima occur in the belt of Ryukyu arc (NAKAMURA and HUNAHASHI, 1970). The belt is characterized by Miocene volcanism which took place probably under the subaerial environment, and Miocene granitic intrusions. The former sometimes follows epithermal gold-silver veins (Taio, Kushikino, and Oguchi deposits), which are closely related to propylitization of intermediate volcanic rocks in the northern and southern Kyushu. The latters often accompany tin and tungsten deposits, and polymetallic veins including large amounts of lead, zinc, copper, arsenic, antimony, tin, and iron sulfide minerals (MIYAHISA, 1960). The ore deposits of this type occur abundantly in the southern Kyushu or Outer Zone of Kyushu, separated by the Usuki-Yatsushiro Tectonic Line. They feature a complex mineralization under a wide range of temperature, *i.e.*, pegmatitic, pneumatolitic, and hydrothermal mineralization or xenothermal one, and are named Obira-type deposits by MIYAHISA (1960).

As the Taishu-type deposit is genetically related to Miocene granite intrusion, it must be compared to the Obira-type deposits. The relation between granite intrusions and ore deposits in Kyushu is summarized as shown in Table 18. Major metals of the Taishu-type is common to those of the Obira-type, but the Obira-type is rich in tin, tungsten, and molybdenum ores. According to spectroanalyses by MUTA (1957a, 1958b), galena and sphalerite ores of the Taishu mine contain a very small amount of tin. Both the types are commonly associated with district zoning around granitic masses, but the Obira-type shows more polyascendent and telescoped mineralizations (NAKAMURA and MIYAHISA, 1976). Therefore, the Taishu-type deposits indicate fairly distinct features in mineralization from those of the Obira-type in the Outer Zone of Kyushu.

On the other hand, the Shigekuma-type deposit is not found in the belt of Ryukyu arc, except Tsushima. However, the Otani deposit, Kagoshima Prefecture, might be regarded a similar deposit. The Otani deposit is a vein-type deposit, yielding copper, lead, zinc, and gold ores, which shows marginal characters of the Obira-type or intermediate with the epithermal gold-silver deposits (MIYAHISA, pers. commun.). The mine was closed in 1943, and detailed mineralization is not known.

It is concluded that the Taishu-type and the Shigekuma-type deposits have rather unique mineralizations in the belt of Ryukyu arc. This is also emphasized by the difference of mineralization features associated with Miocene granite intrusions between the Inner and the Outer Zone of Kyushu. Three masses of

Table 18. Miocene granitic rocks and related ore deposits in Kyushu (modified after MIYAHISA, 1961).

| | Metallogenic sub-province | | Neogene igneous rock | K-Ar Age# | Major metal | Major deposit |
|---|---|---|---|---|---|---|
| Inner Zone of Kyushu | Tsushima | Shigekuma | | | Ag Pb Zn | Shigekuma Nihongi Kanayama |
| | | Taishu | Uchiyama granite | 12 | Pb Zn Fe(S) As Co Bi Te [B] | Himi Shintomi Misoge Ysuda-Taisho Akushidani Senninmabu Ohfunakoshi (pottery stone) |
| | Goto | | granite porphyry | | [B] | (pyrophyllite) |
| | Amakusa | | Tomioka granodiorite | 19 | Sb [B] | (pottery stone) |
| | Taio | | Nakatsue granite | | Au? Ag? | Taio Umeno Mikura Kitamata Tonoo (argillic alteration) |
| Outer Zone of Kyushu | Obira | | Sobosan volcanic complex Okueyama granite | 21 | Sn Zn As Pb Sb Cu W Mn Bi Fe(S) Ag Mo [B] | Obira Hoei Kiura Mitate Nakanouchi Toroku Shishikawa |
| | Matsuo | Ichifusa | Ichifusa granite | 11-14 | Sb As Au Sn | Hibino Shika |
| | | Osuzu | Osuzuyama volcanic complex Kijo granite | 13-15 | As Sn Zn Pb Sb Ag Au Bi Fe(S) [B] | Matsuo Osuzu Oouchi Tsuboya |
| | | Tomitaka | Toomiyama volcanic complex | | Fe(S) Ag Au Sb Mn Zn | Tomitaka Kaneiso Akamizu |
| | Suzuyama | Izumi | Shibisan granite | 13-16 | Sn Sb Zn Pb Cu As | Hiraiwa Izumi Shiraogawa |
| | | Suzuyama | Suzuyama granite porphyry | | Sn Fe(S) As Sb Ag Au [B] | Suzuyama Nishi-Suzuyama Setoyoma Hinomoto Izaku Sukeshiro |
| | | Nomamisaki | Quarz porphyry | | Cu Pb Zn | Noma (Kamishiro) |
| | | Takakuma-yama | Takakumayama granite | 16 | W Mo Au Bi As Sn Fe(S) Sb Ag Au Cu U [B] | Tarumizu Hanaoka Oosumi Togadaira |
| | | Sata | Minami-Osumi granite | 14-22 (64*) | As Au Ag Mo | Sata Ushine |
| | | Yakushima | Yakushima granite | 13-14 | W Mo Au Bi As [B] | Nitta Hayasaki Miyanoura Mochomu Mugio |

#: Kawano & Ueda (1966), Shibata & Nozawa (1966), Shibata & Togashi (1975), *: Rb-Sr whole rock age (Yanagi et al., 1971).

granitic rocks, *i.e.*, Goto, Tomioka, and Taio (or Nakatsue) in the Inner Zone, are poorly related to metalliferous mineralization (Table 18). MIYAHISA (1965) indicated that Neogene metalliferous veins in Kyushu and Shikoku have a tendency that antimony mineralization abounds in the east, and silver in the west. This implies that the site of mineralization in the belt of Ryukyu arc is strongly affected by the mineralization in Setouchi subprovince of the Inner Belt of the Southwest Japan arc, in Neogene age. Similar relation may be expected between North Kyushu and San'in district.

## C. Metallogenic relations between Tsushima and San'in-Hokuriku subprovince

The inner belt of Southwest Japan was a site of intense igneous activity in late Mesozoic, and in some places the activity continued up to Paleogene (Research Group for Late Mesozoic Igneous Activity of Southwest Japan, 1967). Granitic intrusion in late Cretaceous to Paleogene age plays an important role in the formation of the plutonic hydrothermal vein-type deposits and pyrometasomatci deposits in Japan.

San'in-Hokuriku region was a site of violent submarine volcanic activities in Neogene age, and also it took the southern extension of the "Green Tuff region". Mineral deposits in the region can be divided into two genetic groups, one is the Kuroko deposits in middle Miocene age, the stage of subsidence, and the other is the vein-type deposits mainly in late Miocene to early Pliocene age, the stage of general upheaval (TATSUMI *et al.*, 1970).

In the many vein-type deposits in San'in-Hokuriku region, somewhat similar mineral assemblage to that of the Shigekuma-type deposit can be found in the Oomori deposit, Shimane Prefecture. The Oomori deposit produced 65 kg of silver, 1 kg of gold, and 6,300 tons of copper, during 1891 to 1919 (JMIA, 1968). The ores are composed of argentite, chalcopyrite, pyrite, galena, sphalerite, siderite, hematite, quartz, barite, and chalcedony (JMIA, 1968).

Some of the Kuroko deposits in San'in-Hokuriku region show similar mineral assemblage to that of the Shigekuma-type deposit. The Kuroko deposits in the region are not typical, and are mainly composed of network or disseminated ores (DOI and TSUCHIYA, 1970). The Kuroko mineralization occurred in three times during Nishikurosawa and Onnagawa stages (DOI and TSUCHIYA, 1970). In the Iwami deposit, the network ores are developed below the stratabound ores, and are composed of sphalerite, pyrite, chalcopyrite, galena, and small amounts of tetrahedrite and luzonite, associated with quartz and calcite (MUKAIYAMA *et al.*, 1974). Concentration of FeS in sphalerites of the Iwami deposit is as low as 0.2 to 2.6 mol% (URABE, 1974), and homogenization temperature of fluid inclusions mostly ranges from 200° to 250°C (MUKAIYAMA *et al.*, 1974).

Thus the network ores of the Iwami deposit show some similarity to those of the Shigekuma-type. Therefore, the Shigekuma-type deposit in Tsushima may be related to igneous activity and mineralization of the "Green Tuff region". This consideration is supported also by the following things: 1) The

Taishu Group is intruded by rhyolite and dolerite, which are roughly correlated to the same kinds of igneous rocks intruded into the Kuri and Oomori Formations in San'in district. 2) SHIBATA (1967) has suggested that biotite granite of Tsushima belongs to the "Green Tuff-type" in his petrographic classification. 3) According to MUTA (1960), germanium content in sphalerite of Kamishama, Tsushima, shows the similar value to that of the Daira deposit, Akita Prefecture, and some other vein-type deposits, developed in the "Green Tuff" region. 4) "Green Tuff" formations seem to be widely distributed not only in Japan Sea but also in the Sea of Genkai, near the Tsushima Islands, as suggested by FUJITA (1972). 5) URATA (1956) noted that the Nojima Formation in Northwest Kyushu is regarded as the western extension of the "Green Tuff" formations. 6) MATSUMOTO, Y. (1973) stated that "Green Tuff" activities are observed in nine areas in Kyushu, including the Iki Islands.

Accordingly, "Green Tuff" formation equivalent had probably overlaid the Taishu Group, and might have been eroded out, as the degree of compaction of the Taishu Group is assumed to be fairly higher than that of other Tertiarys in Kyushu.

## VI. Concluding remarks

Above investigations of the metalliferous deposits of Tsushima are summarized with some additional remarks, as follows:

The ore deposits are principally fissure-filling veins, composed of lead-zinc-iron sulfides and carbonates. They are distributed in eight areas, and are divided into two distinct types: the Shigekuma-type in Kamishima or North Tsushima, and the Taishu-type in Shimojima or South Tsushima.

Both the types of ore deposits are impregnated in the fractures, having distribution tendency that N-S and NE trending faults are abundant in the western part, and NW ones in the eastern part of the islands.

The host rock is mainly composed of a thick pile of mudstone intercalating sandstone of the Taishu Group, which accumulated in late Oligocene to early Miocene. A tectonic movement was conducted through the "Taishu basin" in early middle Miocene, accompanied by a harmonic correspondence to Takachiho and Mizuho orogenies. It was chiefly initiated and accelerated with the lateral forces having a constant direction of NW-SE. The epoch of lead-zinc mineralizations seems to be middle Miocene.

Shigekuma-type mineralization is characterized mainly by tectonic opening-type zonality, low temperature mineral assemblage (probably under 250°C), and variable chemical composition of major constituent minerals. Hypogene carbonate zoning is found as siderite in and around the ore veins, ankerite in the middle, and calcite in the marginal deeper zone. Around the deposits, no acidic igneous rocks related to mineralization are found. It is considered that the Shigekuma-type deposits were formed under far from the equilibrium condition, accompanied by some phenomena like boiling and throttling.

Taishu-type mineralization shows high temperature mineral assemblage (under 400°C), and gives the keynote of deposition-type zonality or systematic change in composition of minerals with depth. The mineralization is closely related to the 12-million-year-old biotite granite, which crops out at the southern end of Shimojima.

Lead-zinc ore deposits of Tsushima occupy the peculiar situation in the metallogenic belt of Ryukyu arc. There is a possibility that the Shigekuma-type mineralization is genetically related to successive intrusions of dolerite, rhyolite, and cryptobasolith in Kamishima, which may be regarded as a series of "Green Tuff" activity.

Deposits having similar mineral assemblage to those of the Shigekuma-type are scarce in Japan. However, the type fairly corresponds to the mesothermal silver-lead-zinc deposits of LINDGREN, which are of great importance in the Cordilleran region of the United States. The mineral assemblage common to the mesothermal silver-lead-zinc deposits is rather simple. Galena and sphalerite are abundant, and tetrahedrite is common as a silver carrier. The predominant gangue minerals are quartz, siderite, ankerite, and calcite (McKNIGHT, 1933). It may be noted that the Shigekuma-type deposits are very similar in appearance to the deposits in the Coeur d'Alene district, Idaho (SORENSON, 1947; PARK and MACDIAMID, 1964; WARREN HOBBS and FRYKLUND, 1968; LONG *et al.*, 1960), the Onzin deposit, North Korea (WATANABE, 1940), and the Chig-cheng-tzu deposit, Manchuria or Northeast China (TATSUMI, 1942; MATSUDA, 1971).

## *Acknowledgements*

The writer is greatly indebted to Professor Fumitoshi HIROWATARI, Kyushu University, and Professor Emeritus Nobuo KATAYAMA, University of Tokyo, for their continuing guidance and encouragement. He expresses his sincere gratitude to Professor Haruo SHIROZU, Kyushu University, for helpful suggestions and critical reading of the manuscript. He is also grateful to Professors Michitoshi MIYAHISA and Hitoshi MOMOI, Ehime University, who read an early draft of this paper and offered valuable advice.

He greatly thanks to Messrs. Kiyoshi KIRYU, Katsuji FUKUMOTO, and Chosuke KURONUMA, Toho Zinc Company, for permission to use their unpublished maps. Thanks are also due to Drs. Den'ichi SASAKI and Hanzo GOHARA, Messrs. Shuzo MATSUHASHI, Tadashi MAKITA, Yasuo NAKASHIMA, Toru NEMOTO, and other staffs of the Toho Zinc Company, for their kind helps in collecting samples and the field work.

He would express his hearty thanks to Professors Kiyoshi TAKAHASHI and Yukio MATSUMOTO, Nagasaki University, Professor Hakuyu OKADA, Shizuoka University, Dr. Haruo NAGAHAMA, Geological Survey of Japan, Dr. Suzuomi TOMITA, Messrs. Yoshinobu MOTOMURA and Eiji IZAWA, Kyushu University, Dr. Min Sung LEE, Geological and Mineral Institute of Korea, Mr. Shinsei TERASHIMA, Metal Mining Agency of Japan, and Mr. Yoshihiro WATANABE, Dowa Mining Company, for their informative discussions in various phases of this study. The analyses were kindly supported by Mrs. Hidemi AKAMINE, Kyushu University.

A part of the field work for this study was undertaken in aid of grant from the Ministry of Education.

## References cited

BARTON, P. B., Jr. and TOULMIN, P., III. (1966): Phase relations involving sphalerite in the Fe-Zn-S system. *Econ. Geol.*, **61**, 815–849.

BERNARD, J. H. (1957): Investigation of minerals of the tetrahedrite group. *Vestnik Ustr. Ustravu. Geol.*, **32**, 135–145.

DEER, W. A., HOWIE, R. A. and ZUSSMAN, J. (1963): *Rock-forming minerals.* 5, Non-silicates, 2nd ed., 371 p. Longmans, London.

DOI, M. and TSUCHIYA, Y. (1970): Kuroko-type ore deposits in the San'in district, with special reference to the Iwami ore deposits. *Proc. Autumn Mtg., 1960, Mining Metal Inst. Japan,* **I-1**, 1–4 [in Japanese]

FUJITA, Y. (1972): Tectonic movement in the Cenozoic of the Japanese Islands. *Kagaku,* **42**, (4), 212–220 [in Japanese].

Geological and Mineral Institute of Korea (1973): *Geologic map of Korea, in the scale of 1 : 250,000.* 18 sheets.

Geological Research Group of Iki Islands (1973): Geological and paleontological researches of Iki Islands, Japan. *Bull. Japan Sea Resear. Inst., Kanazawa Univ.,* (5), 89–114, 7 pls. [in Japanese with English abstract].

Geological Survey of Japan (1955): *Nihon-Kōsanshi.* **Ia**, 258 p. [in Japanese].

GOLDSMITH, J. R., GRAFT, D. L., WITTERS, J. and NORTHROP, D. A. (1962): Studies in the system $CaCO_3$-$MgCO_3$-$FeCO_3$: 1. phase relations, 2. a method for major element spectrochemical analysis, 3. compositions of some ferroan dolomites. *Jour. Geology,* **70**, 659–688.

HARADA, Z. and KITAHARA, M. (1952): On some sulphosalt minerals (tetrahedrite and tennantite) from Northern Japan. *Jour. Fac. Sci., Hokkaido Univ.,* [IV], (20), 74–81 [in Japanese with English abstract].

HOLLAND, H. D. and BORCSIK, M. (1965): On the solution and deposition of calcite in hydrothermal systems. *Symp; Problem of Postmagmatic Ore Deposition, Prague,* **2**, 364–374.

HOWIE, R. A. and BROADHURST, F. M. (1958): X-ray data for dolomite and ankerite. *Amer. Miner.,* **43**, 1210–1214.

IKEBE, N., TAKAYANAGI, Y., CHIJI, M., CHINZEI, K., IKEBE, Y., NAKASEKO, K. and SHIBATA, K. (1973): Inter-Basial correlation of the Japanese Neogene. *Mem. Geol. Soc. Japan,* (8), 215–219 [in Japanese with English abstract].

IMAI, H. (1967): Genesis and exploration of vein-type ore deposits. *Mining Geology,* **17**, (2–3), 69–70 [in Japanese].

———, TAKENOUCHI, S. and KIHARA, T. (1971): Fluid inclusion study at the Taishu mine, Japan, as related to geological structure. *Soc. Mining Geol. Japan, Spec. Issue,* **3**, 321–326.

——— (1973): The geologic structure and mineralization at the Taishu mine, Nagasaki Prefecture, Japan. *Jour. Mining Metal. Inst. Japan,* **89**, (1026), 509–514 [in Japanese with English abstract].

ISHIBASHI, M. (1953): On the tetrahedrites from some mines in the western Hokkaido (Studies on the major ore minerals, Rept. 4). *Jour. Miner. Soc. Japan,* **1**, 45–50 [in Japanese with English abstract].

IWAO, S. (1958): Taishu kaolin. in SUENO, T. and IWAO, S. ed., *Clay and its utilization,* Asakura, Tokyo, 218–222 [in Japanese].

JMIA (1968): *Nihon-no-kōsho-sōran,* **2**, 941 p., Japan Mining Industry Association [in Japanese].

KATAYAMA, N. (1934): Tetrahedrite crystals from Besshi and Susaki. *Jour. Geol. Soc.*

*Japan*, **41**, 42–43 [in Japanese].
KAWANO, Y. and UEDA, Y. (1966): K-A dating on the igneous rocks in Southwestern Japan. *Jour. Jap. Assoc. Miner. Petr. Econ. Geol.*, **56**, (5), 191–211 [in Japanese with English abstract].
KIM, B. K., NODA, H. and YOON, S. (1974): Molluscan fossils from the Miocene Eoil Formation, Gampo and Ulsan districts, Southeastern-side of Korea. *Trans. Proc. Paleont. Soc. Japan*, [N. S.], (93), 265–285. 2 pls.
KINOSHITA, K. and MUTA, K. (1957): Differentiation of the carbonate minerals in the Chichibu mine, Saitama Prefecture. *Tech. Rep. Kyushu Univ.*, **30**, (1), 48–53 [in Japanese].
KITAMURA, N. (1961): Sole markings in the Taishu Group developed around Mitsu-shima-cho, Tsushima Islands, Japan. *Sci. Rep. Tohoku Univ.*, 2nd Ser., **33**, (1), 105–114, 3 pls.
——— (1962): Preliminary report on systematic jointing in the Taishu Group developed in Mitsushima-cho, Tsushima Islands, Japan. *Sci. Rep. Tohoku Univ.*, 2nd Ser., Spec. vol., (5), 303–319, 1 pl.
KIYOSU, Y. (1973): Sulfur isotopic fractionation among sphalerite, galena and sulfide ions. *Geoch. Jour.*, **7**, 191–199.
KLEMM, D. D. (1965): Synthesen und Analysen in den Dreiecksdiagrammen FeAsS-CoAsS-NiAsS und $FeS_2$-$CoS_2$-$NiS_2$. *N. Jb. Miner. Abh.*, **103**, (3), 205–255.
KULLERUD, G. (1953): The FeS-ZnS system; a geological thermometer. *Norsk. Geol. Tids.*, **32**, 61–147.
KUTINA, J. (1965): The concept of monoascendent and polyascendent zoning. Sym; *Problem of Postmagmatic Ore Deposition, Prague*, **2**, 47–55.
LONG, A., SILVERMAN, A. J. and KULP, J. L. (1960): Isotopic composition of lead and Precambrian mineralization of the Coeur d'Alene district, Idaho. *Econ. Geol.*, **55**, 645–658.
MATSUDA, K. (1971): Silver-lead-zinc deposits in Manchuria. In OGURA, T. ed., *Geology and Mineral Resources of the Far East*, **3**, 100–113.
MATSUHASHI, S. (1967): Structural control and prospecting of the bedding plane veins in the Taishu mine. *Mining Geology*, **17**, (82–83), 151–161 [in Japanese with English abstract].
——— (1968): Analysis of structural control and results of prospecting for bedding-plane veins in the Taishu mine. *Mining Geology*, **18**, (90), 161–172 [in Japanese with English abstract].
———, KIRYU, K., NAKASHIMA, Y., FUKUMOTO, K., NEMOTO, T. and KURONUMA, C. (1970): Geology of the Taishu mine area in Shimo-jima, Tsushima Islands. *Mem. Nat. Sci. Mus. Tokyo*, (3), 1–8 [in Japanese with English abstract].
MATSUMOTO, T., NODA, M. and MIYAHISA, M. (1962): *Nihon-Chiho-Chishitsushi* (Regional geology of Kyushu), 423 p., Asakura, Tokyo [in Japanese].
——— (1969): Geology of Tsushima and relevant problems. *Mem. Nat. Sci. Mus. Tokyo*, (2), 5–18 [in Japanese with English abstract].
MATSUMOTO, Y. (1973): Green Tuff activities in northern and central Kyushu. *Mem. Geol. Soc. Japan*, (9), 153–193 [in Japanese with English abstract].
MATSUO, H. (1971): Paleogene mega-plants remains of the Tsushima Islands, Japan. *Bull. Nat. Sci. Mus. Tokyo*, **14**, (4), 671–710, 10 pls.
MCKNIGHT, E. T. (1933): Mesothermal silver-lead-zinc deposits. In the Committee on the Lindgren Volume ed., *Ore Deposits of the Western States*, 582–602, A.I.M.E.
MINATO, H. and OKAMOTO, Y. (1957): Anatase crystal from the Nariai mine, Tsushima Island, Nagasaki. *Sci. Pap. Coll. Gener. Ed., Univ. Tokyo*, **7**, (1), 145–150.
MITI (Ministry of International Trade and Industry) (1971): *Report on the regional geological survey, Tsushima-Kamiagata district of the 1970's fiscal year.* 29 p. [in Japanese].
——— (1972): *ibid. of the 1971's fiscal year.* 34 p. [in Japanese].

——— (1973): *ibid. of the 1972's fiscal year.* 54 p. [in Japanese].
——— (1974): *ibid. of the 1973's fiscal year.* 52 p. [in Japanese].
——— (1975): *ibid. of the 1974's fiscal year.* 21 p. [in Japanese].
MIYAHISA, M. (1960): Preliminary note on the Cenozoic metallogenic epoch in Kyushu, Japan. *Jour. Mining Inst. Kyushu,* **28**, 127–140 [in Japanese with English abstract].
——— (1961): Geological studies on the ore deposits of Obira-type in Kyushu, (1) General geology and metallogenic provinces. *Jap. Jour. Geol. Geogr.,* **32**, 39–54.
——— (1965): Berthierite-bearing antimony ore deposits in Kyushu and Shikoku. *Tigaku,* **16**, 101–106 [in Japanese with English abstract].
MIYAZAWA, T. (1961): Lowest limit and formation depth of veins. *Mining Geology,* **11**, (45–46), 37–40 [in Japanese].
MUKAIYAMA, H. and MIKURIYA, N. (1964): Occurrence and variation in lattice constant of sphalerite at Taishu Pb-Zn mine, Nagasaki Pref., Japan. *Jour. Mining Inst. Kyushu,* **32**, 202–208 [in Japanese with English abstract].
——— (1965): Variation in Fe-contents and crystal structure of pyrrhotite and sphalerite from the Kunoe deposit of Taishu mine, Nagasaki Pref., Japan. *ibid.,* **33**, 360–367 [in Japanese with English abstract].
——— and IZAWA, E. (1966): Phase relations of pyrrhotite. *ibid.,* **34**, 194–213 [in Japanese with English abstract].
———, MONONOBE, S. and YOSHIDA, T. (1974): Genesis of the ore deposits of the Iwami mine, Shimane Prefecture, Japan. *Mining Geology Spec. Issue,* (6), 221–234.
MURAUCHI, S. (1972): Crustal structure of the Japan Sea derived by explosion seismology. *Kagaku,* **42**, (7), 367–375 [in Japanese].
MUTA, K. (1957a): Distribution of tin in galena from Kyushu. *Tech. Rept., Kyushu Univ.,* **30**, 229–235 [in Japanese].
——— (1957b): On the carbonate minerals associated with ore deposits in Kyushu, (I) and (II). *Jour. Jap. Assoc. Miner. Petr. Econ. Geol.,* **41**, (1), 16–23; (2), 80–87 [in Japanese with English abstract].
——— (1957c): A bismuth-bearing mineral from Naiin, Izuhara town, Nagasaki Prefecture. *Jour. Mining Inst. Kyushu,* **25**, (11), 452 [in Japanese].
——— (1958a): Variation of FeS solubility in sphalerite from Kyushu and its relation with minor elements. *Mem. Fac. Engin., Kyushu Univ.,* **17**, 139–162.
——— (1958b): Minor elements in galena and sphalerite from Kyushu. *Jour. Mining Inst. Kyushu,* **26**, 247–264 [in Japanese with English abstract].
——— (1960): Minor elements in sphalerite from xenothermal deposits. *Jour. Jap. Assoc. Miner. Petr. Econ. Geol.,* **44**, (1), 34–43 [in Japanese].
NAGAHAMA, H., ISOMI, H., ONO, C. and SATO, S. (1966): Dagger blade structure—A new method for detecting line of deposition current of siltstone. *Jour. Geol. Soc. Japan,* **72**, (11), 531–540, 2 pls.
——— (1967): Paleocurrents of the Taishu Group, on the Tsushima Island, Kyushu, Japan. *Jubil. Pub. Prof. Yasuo* SASA, *Sapporo,* 135–144, 2 pls. [in Japanese with English abstract].
——— (1971): Fold structure of the Taishu Group in the northern area of the Tsushima Islands, Kyushu, Japan. *Bull. Geol. Surv. Japan,* **22**, (7), 397–400, 14 pls. [in Japanese with English abstract].
NAGASAWA, K. (1962): Some considerations on the mineralization in the Mikawa mine, Niigata Prefecture. *Mining Geology,* **12**, (54), 211–222 [in Japanese with English abstract].
NAKAMURA, T. and HUNAHASHI, M. (1970): Ore veins of Neogene volcanic affinity in Japan. In TATSUMI, T. ed., *Volcanism and Ore Genesis,* 215–230, Univ. Tokyo Press.
——— and MIYAHISA, M. (1976): Hypogene zoning and role of geologic structures of

vein-type deposits. *Mining Geology Sp. Issue,* (7), 37–57 [in Japanese with English abstract].

NISHIWAKI, C. and SHIOBARA, K. (1948): Native bismuth coexisted in lead-zinc ores (abst.). *Jour. Geol. Soc. Japan,* 54, (693), 184–185 [in Japanese].

———, MATSUKUMA, T. and URASHIMA, Y. (1971): Neogene gold-silver ores in Japan. *Soc. Mining Geol. Japan, Spec. Issue,* 3, 409–417.

OKADA, H. (1960): A preliminary study of the geological section across the northern area of the Tsushima Islands, Kyushu. *Mem. Nat. Sci. Mus. Tokyo,* (2), 19–27, 2 pls. [in Japanese with English abstract].

——— and FUJIYAMA, I. (1970): Sedimentary cycles and sedimentation of the Taishu Group in the Shiohama area, Central Tsushima, Kyushu. *ibid.,* (3), 9–17, 4 pls. [in Japanese with English abstract].

——— (1970): Sedimentation pattern of the lowermost Taishu Group in the Komoda area, South Tsushima, Kyushu. *Sci. Rep., Kagoshima Univ.,* (19), 67–74 [in Japanese with English abstract].

———, SHIBATA, H., TATSUMI, Y. and NABEKURA, N. (1971): Geology of the north-end of Tsushima. *Sci. Rep., Kagoshima Univ.,* (20), 13–31, 7 pls. [in Japanese with English abstract].

OKAMOTO, Y. (1953): New occurrence of mimetite in Tsushima. *Tigaku,* **6,** (4), 207–209 [in Japanese].

——— (1958): *Nagasaki-ken Kōbutsushi* (Description of minerals from Nagasaki Prefecture). Jubil. Pub. Commem. Dr. Yohachiro OKAMOTO, 164 p, Fukuoka [in Japanese].

PALACHE, C., BERMAN, H. and FRONDEL, C. (1944): *Dana's the System of Mineralogy.* 7th ed., 1, 834 p., John Wiley and Sons, New York.

PARK, C. E., Jr. and MACDIAMID, R. A. (1964): *Ore Deposits.* 475 p., Freeman, San Francisco.

PETRUK, W. and staff (1971): Characteristics of the sulphides in the silver-arsenic deposits of the Cobalt Gowganda region, Ontario. *Can. Miner.,* **11,** 196–231, 1 pl.

Research Group for Late Mesozoic Igneous Activity of Southwest Japan (1967): Late Mesozoic igneous activity and tectonic history in the zone of Southwest Japan. *Assoc. Geol. Collaboration; Monograph,* (13), 50 p. [in Japanese with English abstract].

RILEY, J. F. (1974): The tetrahedrite-freibergite series, with reference to the Mount Isa Pb-Zn-Ag ore body. *Miner. Deposita,* **9,** 117–124.

ROSENBERG, P. E. (1967): Subsolidus relations in the system $CaCO_3$-$MgCO_3$-$FeCO_3$ between 350° and 550°C. *Amer. Miner.* **52,** 787–796.

SAKURAI, K. and SUGIYAMA, S. (1943): Pyrargyrite and tetrahedrite from the Unami, Shimane Prefecture. *Jour. Geol. Soc. Japan,* **50,** 101–102 [in Japanese with English abstract].

——— (1957): Morphological study of minerals, Part 3; Cerussite from Tsushima Islands, Nagasaki Prefecture. *Bull. Nat. Sci. Mus. Tokyo,* **3,** (3), 157–159 [in Japanese].

SASAKURA, M. and UEHARA, Y. (1958): Taishu mine. *Ore Deposits and Geological Structures,* (3), 8–12, Mining and Metallog. Inst. Japan [in Japanese].

SATO, T. (1972): Metallogenesis of Neogene base metal and Au-Ag deposits in Japan, with special reference to Kuroko deposits. *Mining Geology Spec. Issue,* (4), 185–203 [in Japanese].

SHAW, H. R. (1959): Phase studies in the Fe-rich carbonates of the Bunker Hill mine, Idaho. *Bull. Geol. Soc. Amer.,* **70,** (9–12), 1674–1675.

SHCHERBAN', I. P. and SHIROKIKH, I. N. (1971): Stability of silica-siderite and silica-ankerite mineral associations under hydrothermal conditions. *Doklady Acad. Nauka, SSSR* (Trans.), **196,** 139–140.

SHIBATA, H. (1967): Tsushima granite. *Nihon-Gansekishi,* **2,** 335–336, Asakura, Tokyo [in Japanese].

SHIBATA, K. and NOZAWA, T. (1966): K-Ar age of granites from Amami-oshima, Ryukyu Islands, Japan. *Bull. Geol. Surv. Japan*, **17**, (7), 430–435 [in Japanese with English abstract .

SHIMADA, N. (1971a): Wall rock alteration associated with lead-zinc ore deposits of the Taishu mine (abst.). *Proc. Assoc. Congr. Jap. Earth Sci. Soc., 1971*, 187 [in Japanese].

——— (1971b): On the occurrence and paragenesis of argentian tetrahedrite from the Shigekuma mine, Tsushima Island, Japan. *Sci. Rep. Dep. Geol., Kyushu Univ.*, **11**, (1), 49–54 [in Japanese with English abstract].

——— and HIROWATARI, F. (1972): Argentian tetrahedrites from the Taishu-Shigekuma mine, Tsushima Island, Japan. *Miner. Jour.*, **7**, (1), 77–87.

——— (1973a): Variation of chemical compositions in ore and gangue minerals in the vein-type deposits—an example of the Taishu-Shigekuma mine. *Proc. Symp; Study on the Formation Temperature of Ore Deposit, 1973*, 18–23 [in Japanese].

——— (1973b): Occurrence and chemical composition of Bi-Te minerals from Yoranaiin, Tsushima Islands (abst.). *Proc. Join Mtgs, Akita*, C17 [in Japanese].

——— and WATANABE, Y. (1973): Ullmannite from the Taishu-Shigekuma mine, Tsushima Islands, Japan. *Sci. Rep. Dep. Geol., Kyushu Univ.*, **11**, (2), 225–229 [in Japanese with English abstract].

SHIROZU, H. (1960): Determination of the chemical composition of chlorites by the X-ray and optical methods. *Jour. Jap. Assoc. Miner. Petr. Econ. Geol.*, **44**, (1), 18–22 [in Japanese with English abstract].

——— (1963): X-ray powder patterns of iron chlorites. *Advances in Cly Science*, **4**, 85–94 [in Japanese with English abstract].

SHUTO, T. (1969): The Takachiho and Green Tuff movement. *76th Congr. Geol. Soc. Japan, Symp; Problems on the Green Tuff*, 15–21 [in Japanese].

SMIRNOV, V. I. (1960): Types of hypogene zonality of hydrothermal ore bodies. *Int. Geol. Congr. Rep., 21st Sess., Norden*, Part **16**, 181–191, Copenhargen.

SORENSON, R. E. (1947): Deep discoveries intensify Coeur d'Alene activities. *Eng. Mining Jour.*, **148**, (10), 70–78.

SUZUKI, Y., YAJIMA, S. and TSUTSUMI, S. (1970): Hakudo and Toseki deposit in the north of Izuhara-machi. *Mem. Nat. Sci. Mus. Tokyo*, (3), 35–44, 3 pls. [in Japanese with English abstract].

TAKAHASHI, K. (1958): *Sabalites* aus den Wakata Schichiten von Tsushima, Nord-kyushu. *Trans. Proc. Paleont. Soc. Japan*, [N. S.], (30), 185–188.

——— (1969): A study of the Taishu Group. *Bull. Fac. Lib. Arts, Nagasaki Univ., Nat. Sci.*, **10**, 67–82 [in Japanese with English abstract].

——— and MATSUHASHI, S. (1970): On the sole marks of the Taishu Group in the Taishu mine and adjacent area. *Bull. Fac. Lib. Arts, Nagasaki Univ., Nat. Sci.*, **11**, 41–52, 1 pl. [in Japanese with English abstract].

——— and NISHIDA, T. (1974): On the molluscan fossils from the lower formation of the Taishu Group in the Kamiagata district of Tsushima Islands. *Bull. Fac. Lib. Arts, Nagasaki Univ., Nat. Sci.*, **15**, 15–20, 1 pl. [in Japanese with English abstract].

TAKENOUCHI, S. (1962): Polyphase inclusions in the quartz from the Taishu mine, Nagasaki Prefecture. *Mining Geology*, **12**, (55), 294–297 [in Japanese with English abstract].

TATEIWA, I. (1934): Cretaceous flora of Tsushima, Japan. *Jap. Jour. Geol. Geogr.*, **11**, (3–4), 185–209.

TATSUMI, T. (1942): On the Honzan deposit of the Ching-cheng-tzu mine, South Manchuria. *Jour. Geol. Soc. Japan*, **49**, 416–425 [in Japanese].

——— (1965): Sulfur isotopic fractionation between coexisting sulfide minerals from some Japanese ore deposits. *Econ. Geol.*, **60**, 1645–1659.

———, SEKINE, Y. and KANEHIRA, K. (1970): Mineral deposits of volcanic affinity in Japan; Metallogeny. In TATSUMI, T. ed., *Volcanism and Ore Genesis*, 3–47, Univ. Tokyo Press.

TERASHIMA, S. and TSUCHIYA, T. (1976): On the regional flexures inferred from gravity data in Tsushima Island. *Mining Geology*, **26**, (3), 191–206 [in Japanese with English abstract].

TOMITA, S., YAMASHITA, A., ISHIBASHI, K., MIKI, T., TAKAHASHI, R., SHUTO, T., URATA, H., HASHIMOTO, I., HONZA, E. and IGARASHI, C. (1975): Submarine geology west of the Tsushima Islands. *Sci. Rep. Dep. Geol., Kyushu Univ.*, **12**, (2), 77–90, [in Japanese with English abstract].

TSUJI, K. (1973): Geology of the Okinoshima in the Sea of Genkai. *Proc. Western Branch, Geol. Soc. Japan*, (57), 3, [in Japanese].

UEHARA, Y. (1959a): On the ore deposits and prospecting in the Taishu mine, Nagasaki Prefecture. *Mining Geology*, **9**, (37), 265–275 [in Japanese with English abstract].

——— (1959b): Exploration at Taishu mine. *Jour. Min. Metal. Inst. Japan*, **75**, (855), 678–683 [in Japanese].

——— and MATSUHASHI, S. (1961): Structural localization of ore shoot at the Taishu mine, Nagasaki Prefecture, Japan. *Mining Geology*, **11**, (45–46), 99–103 [in Japanese with English abstract].

——— (1964): Vertical change of veins with depth and prospecting in the Taishu mine. *Proc. Mtg. 1964, Min. Metal. Inst. Japan*, 72–77 [in Japanese].

URABE, T. (1974): Iron content of sphalerite coexisting with pyrite from some Kuroko deposits. *Mining Geol. Spec. Issue*, (6), 377–384.

URATA, H. (1956): A propos du plus haut range de ⟨⟨la Serie de Nozima⟩⟩. *Rep. Earth Sci. Dep. Gener. Educ., Kyushu Univ.*, (2), 47–56 [in Japanese with French abstract].

USHIZAWA, N. (1969): State of silver minerals in ores and products with ore dressing. *Jour. Min. Metal. Inst. Japan*, **85**, (976), 648–651 [in Japanese].

WARREN HOBBS, S. and FRYKLUND, V. C., Jr. (1968): The Coeur d'Alene district, Idaho. In RIDGE, J. D. ed., *Ore Deposits of the United States, 1933–1967*. The Graton-Sales Volume, **2**, 1417–1435, A.I.M.E.

WATANABE, T. (1940): The occurrence and distribution of gold and silver in the ore of the Onzin mine, Korea. *Jour. Jap. Assoc. Miner. Petr. Econ. Geol.*, **23**, 103–114 [in Japanese].

——— (1943): Mode of occurrence of minerals of the enargite group from the Teine mine, Hokkaido. *ibid.*, **30**, 74–84 [in Japanese].

WATANABE, Y. (1972MS): Geology and ore deposits of the Taishu-Shigekuma mine, Tsushima Islands. *Graduation Thesis, Fac. Sci., Kyushu Univ.* [in Japanese with English abstract].

WU, I. J., PETERSEN, U. and HOLLAND, H. D. (1974): Tetrahedrite-tennantite at Casapalca, Peru, and its application to mineral exploration. *Geol. Soc. Ann. Mtg., Abst.*

YAMAOKA, K. (1969): On the gold-silver minerals in the Kuroko deposits, northern Japan. *Symp; Constituent Minerals of Kuroko deposits, and Crystallography and Geochemistry of Sulfide minerals from Hydrothermal Depoists*, 1–37 [in Japanese].

——— (1976): On the genetical problems of the vein-type deposits of the Neogene age in the Inner belt of Northeast Japan. *Mining Geology Sp. Issue*, (7), 59–74 [in Japanese with English abstract].

YANAGI, T., YAMAGUCHI, M. and NOZAWA, T. (1971): Rb-Sr whole rock ages of the granites of Minami-osumi and Amami-oshima, Southwest Japan. *Mem. Fac. Sci., Kyushu Univ.*, [D], **21**, 163–175.

YUI, S. (1971): Heterogenity within a single grain of minerals of the tennantite-tetrahedrite series. *Soc. Mining Geol. Japan, Spec. Issue*, **2**, 22–29.

# Appendix

| | |
|---|---|
| Ajiro | 網代 |
| Akushidani | 悪水谷 |
| Amanohara | 天の原 |
| Aré | 阿連 |
| Chihira | ちひら |
| Ching-cheng-tzu | 青城子 |
| Chubu | 中部 |
| Furukawa | 古川 |
| Gozaemon | 五左衛門 |
| Genju-Nakinaki | 源汁ナキナキ |
| Hazami | 波佐見 |
| Hikage | 日掛 |
| Himi | 日見 |
| Honpi | 本銿 |
| Iguchihama | 井口浜 |
| Iki | 壱岐 |
| Izuhara | 厳原 |
| Kaidokoro | 飼所 |
| Kamisaka | 上見坂 |
| Kamishima | 上島 |
| Kanayama | 金山 |
| Kasayama | 笠山 |
| Kashine | 樫根 |
| Katsumoto | 勝本 |
| Kechi | 鶏知 |
| Kin | 琴 |
| Koenosaka | 越坂 |
| Komoda | 小茂田 |
| Konjobana | 紺青鼻 |
| Koonokiyama | 香木山 |
| Kotsuki | 上槻 |
| Kune-Toobu | 久根東部 |
| Kunoe | 久野恵 |
| Kuroshima | 黒島 |
| Kushi | 櫛 |
| Kushikino | 串木野 |
| Maetake | 前岳 |
| Miné | 峰 |
| Miné-Kanayama | 三根金山 |
| Misaki | 御崎 |
| Misoge | みそげ |
| Misumiyama-Higashi | 三隅山東 |
| Miyama-Shigeeda | 深山茂枝 |
| Momijiyama | 紅葉山 |
| Motoyamamichi | 元山道 |
| Nariaisai | 成相[illegible] |
| Nakanosae | 中之[illegible] |
| Nezumijima | 鼠島 |
| Nihongi | 二本木 |
| Nishikura | 西倉 |
| Nishizawa | 西沢 |
| Nita-Miné | 仁田・峰 |
| Ogata | 緒方 |
| Oguchi | 大口 |
| Ohfunakochi | 大船越 |
| Okinoshima | 沖の島 |
| Okutomi | 億富 |
| Onzin | 甕津 |
| Oomori | 大森 |
| Otani | 大谷 |
| Otedo | オテド |
| Ozakiyama | 尾崎山 |
| Sago | 佐護 |
| Saka | 佐賀 |
| San'ei | 三栄 |
| Sasu | 佐須 |
| Seibu | 西部 |
| Sekinokuma | 関の隈 |
| Senninmabu | 千人間歩 |
| Seo-gui-po | 西帰浦 |
| Seta | 瀬田 |
| Shigekuma | しげくま |
| Shiine | 椎根 |
| Shiinehama | 椎根浜 |
| Shikoe | 志越 |
| Shimobaru | 下原 |
| Shimojima | 下島 |
| Shimoken | 下県 |
| Shinsaka | 新坂 |
| Shintomi | 新富 |
| Shiohama | 塩浜 |
| Shiratake | 白岳 |
| Shiratake-Uwaban | 白岳上盤 |
| Shirogane | 白銀 |
| Shitaban | 下盤 |
| Showa | 昭和 |
| Somen | 層面 |
| Sumo | 洲藻 |
| Taihei | 太平 |
| Taio | 鯛生 |
| Taishu | 対州 |
| Taishu-Shigekuma | 対州しげくま |
| Toho | 東邦 |
| Tonohama | 殿浜 |
| Tsurue | 鶴恵 |
| Tsuruketa | 鶴桁 |
| Tsushima | 対島 |
| Tsutsu | 豆酘 |
| Urakochi | 裏河内 |
| Uwaban | 上盤 |
| Wakata | 若田 |
| Yang-bug | 陽北 |

| | | | |
|---|---|---|---|
| Yasuda-Taisho | 安田・大正 | Yoranaiin | 与良内院 |
| Yeong-il | 迎 日 | Yoshiki | 吉 城 |
| Yora | 与 良 | | |